# ARAP2 effects on the actin cytoskeleton are dependent on Arf6-specific GTPase-activating-protein activity and binding to RhoA-GTP

**Hye-Young Yoon[1], Koichi Miura[1,*], E. Jebb Cuthbert[2], Kathryn Kay Davis[2], Bijan Ahvazi[3], James E. Casanova[2] and Paul A. Randazzo[1,‡]**

[1]Laboratory of Cellular Oncology, Center for Cancer Research, National Cancer Institute, Department of Health and Human Services, Building 37, Bethesda, MD 20892, USA
[2]Department of Microbiology, University of Virginia at Charlottesville, School of Medicine, Charlottesville, VA, USA
[3]X-Ray Crystallography Facility, Office of Science and Technology, National Institute of Arthritis and Musculoskeletal and Skin Disease, National Institutes of Health, Bethesda, MD, USA

*Present address: Osaka Bioscience Institute, 6-2-4 Furuedai, Suita,Osaka 565-0874, Japan
‡Author for correspondence (e-mail: randazzo@helix.nih.gov)

*Accepted 31 August 2006*
*Journal of Cell Science 119, 4650-4666 Published by The Company of Biologists 2006*
*doi:10.1242/jcs.03237*

## Summary

**ARAP2 is a protein that contains both ArfGAP and RhoGAP domains. We found that it is a phosphatidylinositol (3,4,5)-trisphosphate-dependent Arf6 GAP that binds RhoA-GTP but lacks RhoGAP activity. In agreement with the hypothesis that ARAP2 mediates effects of RhoA, endogenous ARAP2 associated with focal adhesions (FAs) and reduction of ARAP2 expression, by RNAi, resulted in fewer FAs and actin stress fibers (SFs). In cells with reduced levels of endogenous ARAP2, FAs and SFs could be restored with wild-type recombinant ARAP2 but not mutants lacking ArfGAP or Rho-binding activity. Constitutively active Arf6 also caused a loss of SFs. The Rho effector ROKα was ineffective in restoring FAs. Conversely, overexpression of ARAP2 did not restore SFs in cells treated with a ROK inhibitor but induced punctate accumulations of paxillin. We conclude that ARAP2 is an Arf6GAP that functions downstream of RhoA to regulate focal adhesion dynamics.**

Key words: Actin, Rho, Arf, GTPase-activating protein

## Introduction

The regulated movement of cells is crucial to development and normal physiology and contributes to pathological processes such as invasion and metatasis in cancer (Geho et al., 2005; Webb et al., 2002). Movement involves the formation and remodeling of structures including focal adhesions (FAs), actin stress fibers (SFs), filopodia and lamellipodia (Schwartz and Ginsberg, 2002; Webb et al., 2002; Nobes and Hall, 1995; Fukata et al., 2001; Demali et al., 2003; Shattil and Newman, 2004). The signaling cascades necessary for coordination of the underlying biochemical activities involve transmembrane receptors, such as integrins, Arf and Rho family GTP-binding proteins and their regulators, including Arf-GTPase-activating proteins (GAPs) and RhoGAPs (Turner et al., 2001; Schwartz and Ginsberg, 2002; Webb et al., 2002; Demali et al., 2003; Shattil and Newman, 2004; Peck et al., 2002; Nie et al., 2003; Randazzo and Hirsch, 2004; Randazzo et al., 2000a).

Rho family GTP-binding proteins are crucial regulators of the actin cytoskeleton. Rho proteins function downstream of integrins but can also affect integrin activation (Fukata et al., 2001; Ridley, 2001; Nobes and Hall, 1995; Hall, 1998). Twenty Rho family GTP-binding proteins have been identified. Of these, RhoA, Rac1 and Cdc42 are the best characterized and have been implicated in the regulation of specific cytoskeletal structures (Nobes and Hall, 1995; Ridley, 2001; Hall, 1998). RhoA regulates the formation of actin SFs and FAs (Hall, 1998). Two primary effectors have been identified that mediate these activities, mDia and Rho-kinase (ROKα) (Leung et al., 1996; Amano et al., 1997; Nakano et al., 1999; Watanabe et al., 1999). mDia is a formin-homology protein that is activated by RhoA-GTP to promote the polymerization of actin filaments. ROKα has a number of substrates, including myosin light chain, myosin light-chain phosphatase and LIM-kinase, that affect actin SFs and FA formation (Kimura et al., 1996; Maekawa et al., 1999).

Arf family GTP-binding proteins regulate both actin remodeling and membrane trafficking (Moss and Vaughan, 1998; Nie et al., 2003; Randazzo et al., 2000a; Donaldson and Jackson, 2000). The six mammalian Arf proteins can be divided into three classes: class 1 with Arf1, Arf2 and Arf3; class 2 with Arf4 and Arf5; and class 3 with Arf6. Arf1 and Arf6 are the most extensively studied. A role for Arf1 in membrane trafficking is well established (Rothman, 2002; Randazzo et al., 2000a; Nie et al., 2003). Although concentrated in the Golgi and on endosomal membranes, Arf1 has also been shown to regulate FA dynamics (Norman et al., 1998). Unlike Arf1, Arf6 is distributed primarily in the periphery where it associates with the plasma membrane and endosomal compartments. Arf6 affects both membrane traffic and cytoskeleton organization (Donaldson, 2003). Arf family proteins do not have detectable intrinsic GTPase activity; consequently GTPase-activating proteins (GAPs) are crucial for Arf function (Randazzo and Kahn, 1994; Nie et al., 2003). The ArfGAPs are a family of proteins with diverse domain

structures (Randazzo and Hirsch, 2004; Turner et al., 2001). Twenty-four genes encoding proteins with an ArfGAP domain have been identified. Three types of ArfGAPs have been implicated in the regulation of the actin cytoskeleton. One ArfGAP, GIT, binds to paxillin and is thought to function as a scaffold at FAs (de Curtis, 2001; Turner et al., 2001). Another ArfGAP, ASAP1, binds to Src, focal adhesion kinase (FAK) and CrkL, three proteins important to FA function and cell motility (Brown et al., 1998; Liu et al., 2002; Liu et al., 2005; Oda et al., 2003) and associates with and regulates FAs (Randazzo et al., 2000b; Liu et al., 2002; Liu et al., 2005; Furman et al., 2002). The ARAPs are a third type of ArfGAP implicated in the regulation of actin and cell motility (Stacey et al., 2004; Miura et al., 2002; Krugmann et al., 2002).

There are three genes for ARAPs, ARAP1, ARAP2 and ARAP3. The first two were identified by homology with other ArfGAPs (Miura et al., 2002). ARAP3 was identified in a screen for phosphatidylinositol (3,4,5)-trisphosphate [PtdIns(3,4,5)P3]-binding proteins (Krugmann et al., 2002) and in a screen for proteins phosphorylated by Src (Stacey et al., 2004). The ARAPs have a complex domain structure (Fig. 1A), including a sterile α-motif (SAM) at the extreme N-terminus, five PH domains, ArfGAP, RhoGAP and Ras-association (RA) domains. Characterization of ARAP1 and ARAP3 has been reported (Krugmann et al., 2002; Stacey et al., 2004; Miura et al., 2002). Both have PtdIns(3,4,5)P3-dependent ArfGAP activity and overexpression of either protein alters the organization of the actin cytoskeleton. ARAP1 is associated with the Golgi complex, whereas ARAP3 is cytosolic with some association with the cell edge.

Here, we report the characterization of a third ARAP protein, ARAP2. One feature that distinguishes ARAP2 from other ARAPs is that it contains a glutamine in place of the arginine thought to be crucial for RhoGAP activity. We found that, rather than functioning as a RhoGAP, ARAP2 binds RhoA and mediates at least part of RhoA function in the formation of FAs.

## Results

ARAP2 is similar to ARAP1 and ARAP3 in that it contains both ArfGAP and RhoGAP domains (Schematic in Fig. 1A) but is distinguished in that the RhoGAP domain contains a glutamine in place of the arginine that is presumed to be catalytic. Here, we have characterized the biochemical properties of the two GAP domains in ARAP2.

### ArfGAP activity of ARAP2

To examine the ArfGAP domain of ARAP2, a recombinant protein comprising the domains PH1, PH2, ArfGAP and ANK repeats of ARAP2 (amino acid residues 467-930) was expressed in HEK 293 cells and purified by immunoprecipitation or by immunoprecipitation followed by affinity purification on a PtdIns(3,4,5)$P_3$ column (Fig. 1B). Similar results were obtained with either preparation. First, ARAP2 was titrated into reactions containing a mixture of phospholipids that supported optimum activity, such as phosphatidic acid (PA), phosphatidylinositol (4,5)-bisphosphate [PtdIns(4,5)$P_2$] and PtdIns(3,4,5)$P_3$, and either Arf1, Arf5 or Arf6 to identify the most efficient substrate (Fig. 1C). Arf6 was the preferred substrate over Arf5 and Arf1, although there was activity with all three proteins. For other ArfGAPs, an arginine within the ArfGAP domain was crucial for activity. A mutant with lysine in place of arginine 728 had no detectable activity (not shown).

The lipid dependency of the GAP activity of ARAP2 was determined using Arf6 as a substrate (Fig. 1D,E). Of the phospholipids examined, greatest activation was seen with PtdIns(3,4,5)$P_3$ and PtdIns(4,5)$P_2$ (Fig. 1D). Phospholipids presented in combination stimulated GAP activity to a greater extent than phospholipids presented alone. For instance, the presence of 10 μM PtdIns(4,5)$P_2$ decreased the requirement of PtdIns(3,4,5)$P_3$ for activity by approximately fivefold (Fig. 1E).

To define Arf specificity in intact cells, the effect of overexpression of ARAP2 on the localization of Arf1, Arf5 and Arf6 in U118 glioblastoma cells was determined (Fig. 1F). In non-transfected cells (i.e. with endogenous levels of ARAP2), Arf1 was found in a perinuclear distribution characteristic of the Golgi complex. Arf5 was diffusely distributed, with a fraction at or near the plasma membrane. The distribution of Arf1 and Arf5 was not detectably different in cells overexpressing ARAP2 compared with cells expressing only endogenous protein. By contrast, Arf6, which is normally associated with the plasma membrane, was shifted from the cell edge. A point mutant of ARAP2 ([R782K]ARAP2) lacking GAP activity did not affect the distribution of Arf6 to the same extent but, instead, colocalized with Arf6 at the cell edge. The effects of ARAP2 on Arf6 distribution were quantified by measuring signal intensity in 50×10 pixel rectangles drawn over the cell edge or inside the cell border, not including the edge. The values were consistent with the qualitative assessment (see Table 1).

As a second test for Arf specificity, U118 glioblastoma cells overexpressing ARAP2 with different Arf isoforms were treated with tetrafluoroaluminate ($AlF_4$), which stabilizes a complex of Arf-GDP with ArfGAPs (Klein et al., 2005; Jackson et al., 2000; Nie et al., 2006) (Luo and P.A.R., manuscript in preparation). In cells coexpressing Arf6 and ARAP2, Arf6 is not associated with the cell edge. Upon treatment with $AlF_4$, Arf6 was found at the cell edge colocalized with overexpressed ARAP2 (Fig. 1G, right group of panels). Arf1 and Arf5 were not affected (Fig. 1H).

The effect of ARAP2 on in vivo levels of activated Arfs was also determined (Fig. 1I). In these experiments, Arf1 and Arf6 were coexpressed with ARAP2, Arf1-specific AGAP1 or Arf6-specific ACAP1. Cells were lysed, activated Arf was co-precipitated with GST-GGA and precipitated Arf was detected by immunoblotting as described (Santy and Casanova, 2001; Yoon et al., 2005). ARAP2 overexpression caused a reduction in Arf6-GTP levels but had no effect on Arf1-GTP. As anticipated, Arf1-GTP levels were reduced by the Arf1GAP AGAP1 and Arf6-GTP levels were reduced by ACAP1. On the basis of these results, we conclude that ARAP2 is an Arf6-specific GAP.

### ARAP2 interaction with Rho family proteins

The RhoGAP domain of ARAP2 lacks the catalytic arginine residue that is crucial for activity in all other RhoGAPs so far examined. To determine whether ARAP2 retains GAP activity for the Rho family GTP-binding proteins RhoA, Rac1 and Cdc42, we first measured activity in an in vitro assay. Although we were able to detect GAP activity against Cdc42 with the

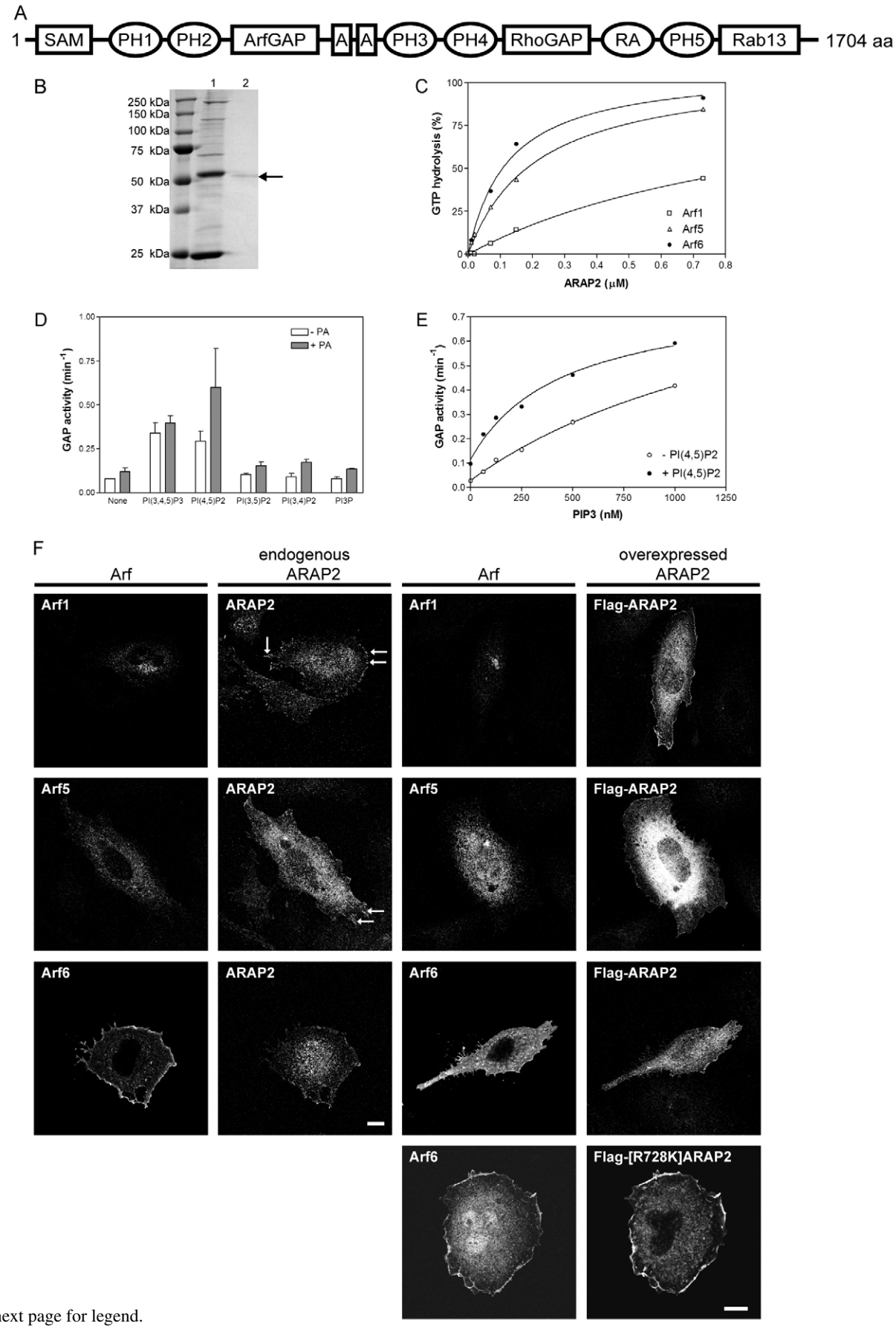


**Fig. 1.** See next page for legend.

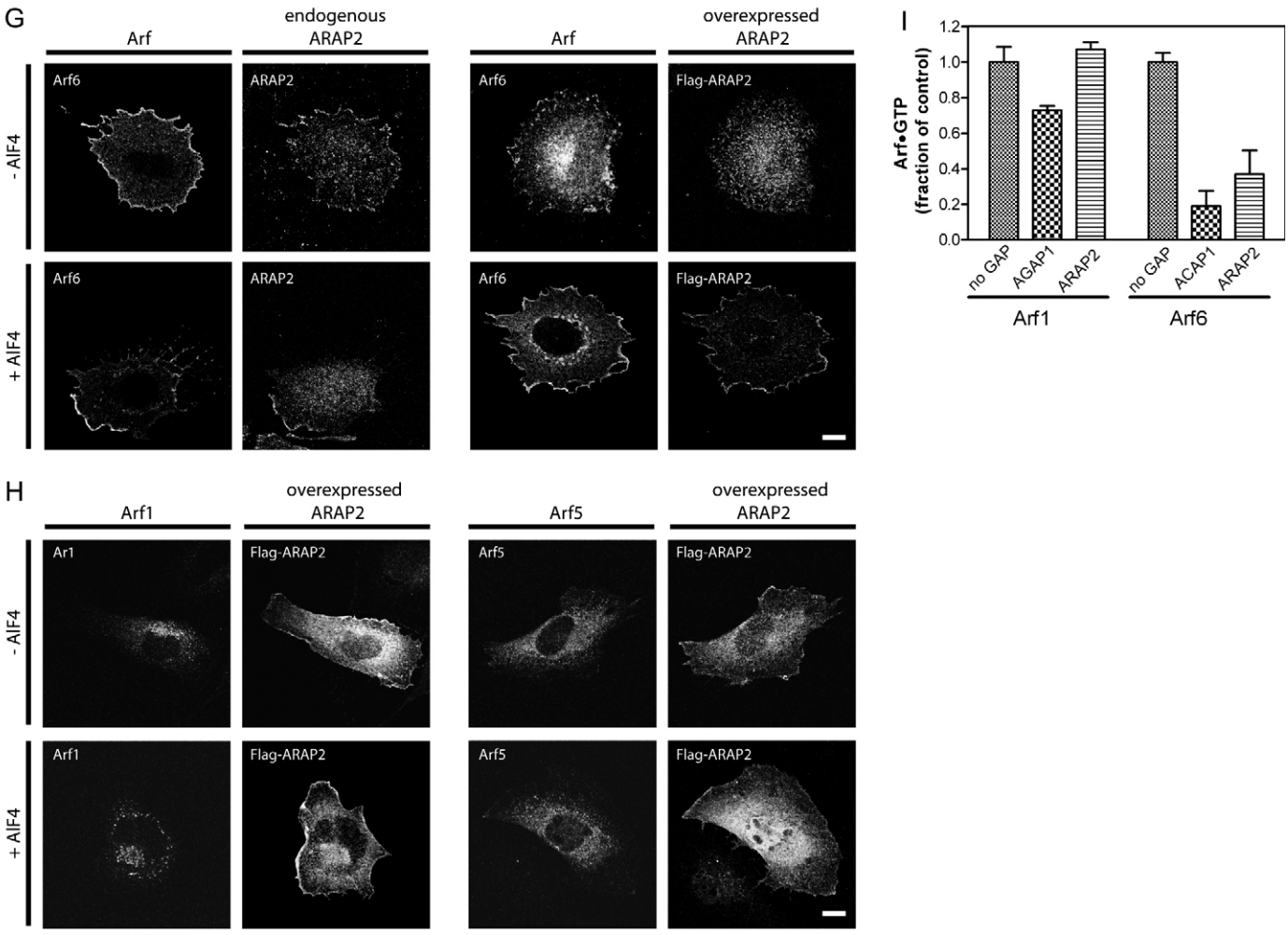


**Fig. 1.** Characterization of the ArfGAP activity of ARAP2. (A) Schematic representation of ARAP2. ARAP2 accession no. NM_015230. SAM, sterile α-motif; PH, pleckstrin-homology domain; ArfGAP, ArfGTPase-activating protein; RhoGAP, RhoGTPase-activating protein; A, ankyrin repeat; RA, Ras-associating domain; and Rab13, Rab13 effector. (B) Purification of recombinant ARAP2. Flag[467-930]ARAP2 was expressed in HEK 293 cells and purified by immunoprecipitation (lane 1) or immunoprecipitation followed by affinity purification on a PtdIns(3,4,5)$P_3$ column (lane 2). The arrow points to [467-930]ARAP2 separated on a polyacrylamide gel. (C) In vitro Arf specificity of ARAP2. The ArfGAP assay was performed in the presence of 50 μM PA, 10 μM PtdIns(4,5)$P_2$, 100 nM PtdIns(3,4,5)$P_3$, with Arf1-GTP, Arf5-GTP or Arf6-GTP as substrate, and the indicated amount of purified ARAP2 (μM). (D) Activation of ArfGAP activity by PtdIns. The ArfGAP activity was measured as in the presence of 100 nM PtdIns(3,4,5)$P_3$ [PI(3,4,5)P3], 10 μM PtdIns(4,5)$P_2$ [PI(4,5)P2], 500 nM PtdIns(3,5)$P_2$ [PI(3,5)P2], 500 nM PtdIns(3,4)$P_2$ [PI(3,4)P2] or 500 nM PtdIns(3)$P$ [PI(3)P] with or without 50 μM PA. Arf6 was used as a substrate. (E) Activation of ARAP2 ArfGAP activity by mixtures of PtdIns(3)$P$ and PtdIns(4,5)$P_2$. The ArfGAP assay was performed in the presence of varying concentration of PtdIns(3)$P$ (PIP3) and in the absence (+) or presence (–) of 10 μM PtdIns(4,5)$P_2$ [PI(4,5)P2]. (F) Localization of ARAP2 relative to and effect of overexpressed ARAP2 on epitope-tagged Arf proteins. U118 cells were transfected with plasmids encoding HA-tagged Arfs and, where indicated, Flag-tagged ARAP2, and stained with rabbit polyclonal Ab against ARAP2 or against the epitope tag and mouse monoclonal Ab to the HA-epitope followed by Texas-Red-conjugated anti-rabbit IgG and fluorescein-conjugated anti-mouse IgG. Arrows indicate endogenous ARAP2. Bars, 10 μm. (G,H) Effect of tetrafluoraluminate on relative ARAP2 and Arf6 (G) and Arf1 and Arf5 (H) localization. Where indicated, U118 cells expressing Arf6-HA, Arf1-HA or Arf5-HA and Flag-ARAP2 were treated with $AlF_4^-$ for 10 minutes, fixed and stained. Bars, 10 μm. (I) The effect of ARAP2 on in vivo Arf-GTP. Arf1 and Arf6 were coexpressed with ARAP2, AGAP1 or ACAP1. Cells were lysed and activated Arf was co-precipitated with GST-GGA. The precipitated Arf was detected by immunoblotting with monoclonal anti-HA Ab.

positive control ARAP1, we did not detect activity using a recombinant protein consisting of PH3, PH4, RhoGAP and RA domains of ARAP2 with Cdc42 (Fig. 2A), Rac1 or RhoA (not shown) as a substrate. We then examined the effect of overexpressing ARAP2 on RhoA-GTP, Rac1-GTP and Cdc42-GTP levels in cells using GST-Rhotekin-RBD to precipitate RhoA-GTP (Fig. 2B,E) and GST-PAK-RBD to precipitate Cdc42-GTP (Fig. 2C) and Rac1-GTP (Fig. 2D). In these experiments, p190RhoGAP (Settleman et al., 1992) was used as a positive control for RhoA. With the two proteins expressed to similar extents, p190RhoGAP reduced RhoA-GTP levels, whereas ARAP2 overexpression increased the levels of RhoA

**Table 1. Relative distribution of Arf1 in cells overexpressing ARAP2**

| Protein expressed | Edge to cytoplasm intensity ratio |
|---|---|
| Control | 2.3±0.8 |
| ARAP2 | 0.52±0.58* |
| [R728K]ARAP2 | 1.7±0.8 |

Cells expressing Arf6-HA with or without Flag-ARAP2 were immunostained for Arf6 and ARAP2. Images were obtained by confocal microscopy. Three to four regions of interest (ROI) were assigned on the membrane and nearby cytoplasm for each cell analyzed. The pixel size of all ROIs was the same, 50×10 pixels. The mean ± standard deviation of the ratio of fluorescence intensity at the edge to the intensity in the cytoplasm is presented.

(Fig. 2B,E) and had no detectable effect on Rac1 or Cdc42 (Fig. 2C,D). Overexpression of the mutant [R728K]ARAP2, which lacks ArfGAP activity, also increased RhoA-GTP levels (Fig. 2E). On the basis of these results, we conclude that ARAP2 lacks RhoGAP activity.

Given the precedent of other proteins with GAP domains that do not have GAP activity but do bind Rho family proteins (Faucherre et al., 2003; Zheng et al., 1994), the ability of ARAP2 to bind to RhoA, Rac1 and Cdc42 was determined. HEK 293 cells were co-transfected with plasmids directing the expression of Flag-tagged ARAP2 and either RhoA, Rac1 or Cdc42, each containing the AU5 epitope tag. The cells were lysed and protein immunoprecipitated through the Flag epitope. In addition to ARAP2, precipitates contained RhoA but not Rac1 or Cdc42 (Fig. 2F).

To determine whether RhoA binding to ARAP2 is dependent on the nucleotide bound to RhoA, GST-RhoA adsorbed to glutathione beads was loaded with GTPγS or GDPβS. The immobilized RhoA was then incubated with lysates of cells expressing ARAP2 and precipitated by centrifugation. The amount of ARAP2 that precipitated with RhoA was determined by immunoblotting. As shown in Fig. 2G, ARAP2 was detected in precipitates containing GST-RhoA–GTPγS but little or none was present in precipitates with either GST-RhoA–GDPβS or GST alone.

ARAP2 has several domains that could bind to RhoA, including the RA domain and the RhoGAP domain. To determine which site binds RhoA, we expressed recombinant proteins comprising isolated domains of ARAP2 in HEK 293 cells. Lysates of these cells were mixed with GST-RhoA–GTPγS, proteins were precipitated with glutathione beads and the presence of recombinant ARAP2 in the precipitates was detected by immunoblotting (Fig. 2H). We found that the isolated RhoGAP domain precipitated with GST-RhoA–GTPγS. Little or no protein containing the RA domain or a protein comprising PH1, PH2, ArfGAP and Ank repeat domains was detected in the precipitates. We next introduced a mutation into ARAP2 that would result in incorporation of a proline in place of lysine 1190. Based on homology modeling of the RhoGAP domain, switch I and switch II of RhoA fit into a slot formed by two α-helices of the RhoGAP domain (Fig. 2K) (Rittinger et al., 1997a; Rittinger et al., 1997b). Lysine 1190 of ARAP2 is within one of the α-helices and is in contact with aspartate 65 in switch II of RhoA. A proline in position 1190 would disrupt this interaction and introduce a kink into the helix, further disrupting the intramolecular contact. Whereas the mutant of ARAP2, [R728K]ARAP2, precipitated as efficiently as wild-type ARAP2 (Fig. 2I), [K1190P]ARAP2 did not bind to RhoA-GTP, supporting the idea that the RhoGAP domain mediates binding (Fig. 2J).

**Fig. 2.** Interaction between ARAP2 with Rho family GTP-binding proteins. (A) In vitro tests for RhoGAP activity of ARAPs. The GAP activity of ARAP1 and Flag-tagged [875-1704]ARAP2 using His-tagged Cdc42 as a substrate was measured. (B-D) Effect of ARAP2 on in vivo levels of (B) RhoA-GTP, (C) Cdc42-GTP and (D) Rac1-GTP. ARAP2 or p190RhoGAP were expressed with RhoA-AU5, Cdc42-AU5 or Rac1-AU5, as indicated, in HEK 293 cells. RhoA-GTP, Cdc42-GTP and Rac1-GTP levels were measured by co-precipitation with GST-Rhotekin-RBD-coated beads (for RhoA) or GST-PAK-PBD-coated beads (for Cdc42 and Rac1) followed by immunoblotting. Expression levels of RhoA, Cdc42, Rac1, ARAP2 or p190RhoGAP in the total cell lysates are shown. (E) Quantitation of RhoA-GTP levels in cells expressing ARAP2. The experiment described in B was repeated and signals were quantified with a scanning densitometer. The results presented are normalized to the levels of RhoA-GTP in the absence of RhoGAP or ARAP2 and are the means and range of duplicate determinations. (F) Binding of Rho family proteins to ARAP2 in vivo. HEK 293 cells were co-transfected with ARAP2 and either AU5-tagged RhoA, Rac1, or Cdc42. Proteins were immunoprecipitated using anti-FLAG M2 gel. Co-precipitated Rho family proteins were detected by immunoblotting with an anti-AU5 Ab. Protein expression levels in the total cell lysates is shown. (G) Nucleotide dependence of Rho binding to ARAP2. Lysates of HEK 293 cells transiently expressing ARAP2 were incubated with GSTRhoA loaded with 100 μM GDPβS or GTPγS or with GST. (H) Identification of the ARAP2 domain that interacts with RhoA. GST-RhoA–GTPγS or GST was incubated with lysates of HEK 293 cells transfected with expression constructs encoding Flag-tagged fragment corresponding to amino acids 467-930 (PH1-ANK domain), 1114-1323 (RhoGAP domain), 1317-1433 (RA domain) of ARAP2. The amount of Flag-tagged protein co-precipitating with GST or GST-RhoA immobilized on beads was determined by immunoblotting. Expression levels of GST or GST-RhoA and the recombinant Flag tagged ARAP2 are shown. (I) Effect of changing arginine 728 to lysine on ARAP2 binding to RhoA. Lysates from cells expressing Flag-ARAP2 or Flag-[R728K]ARAP2 were incubated with GST-RhoA–GTPγS or GST as a control, and interaction was determined as described in (F) and (G). A Coomassie-blue-stained acrylamide gel electrophoresis fractionation of GST and GST-RhoA. The levels of recombinant ARAP2 proteins in the cell lysates was determined by immunoblotting. (J) Effect of changing lysine 1190 to proline on ARAP2 binding to RhoA. Lysates from cells expressing Flag-ARAP2 or Flag-[K1190P]ARAP2 were incubated with GST or GST-RhoA–GTPγS. The experiment was performed as described in (I). (K) Model of ARAP2 RhoGAP domain and predicted consequences of mutating lysine 1190 to proline. Ribbon image of the structure of the Rho-GDP-$AlF^-_4$ (purple)–RhoGAP (green) complex. The $Mg^{2+}$ ion is shown in gray and the GDP molecule and $AlF^-_4$ are shown in ball-and-stick. The Asp side chains from switch II and a conserved lysine residue in RhoGAP protein are shown in the left panel. The lysine to proline mutation residue is highlighted in the right panel. The panel in the center is an enlarged view of salt-bridging interactions between Asp63 from the switch II region with the conserved lysine (proline mutation) residue in RhoGAP protein.

## ARAP2 affects focal adhesion and stress fibers

To identify the site of ARAP2 action, we first determined the localization of endogenous ARAP2 by immunostaining (see

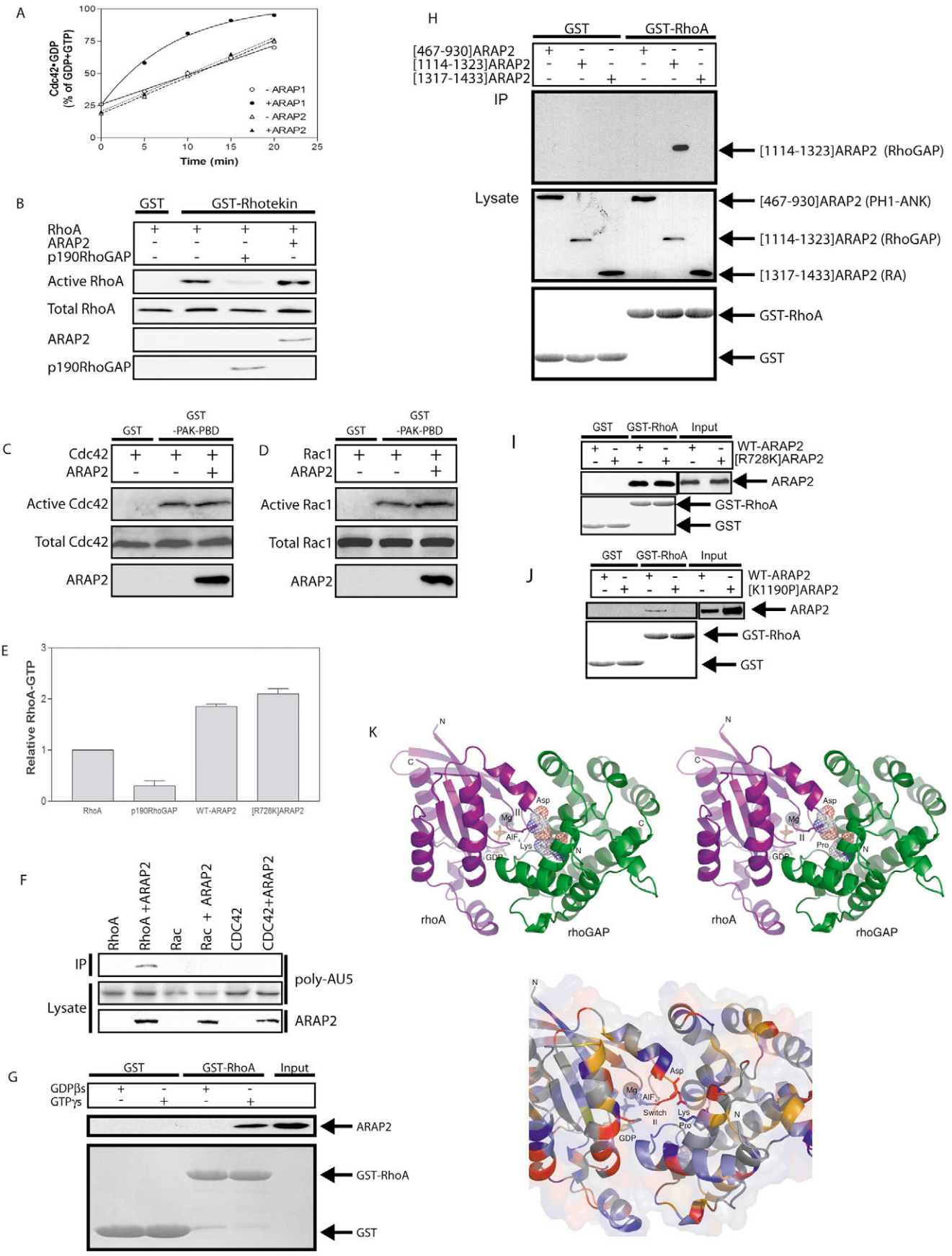


**Fig. 2.** See previous page for legend.

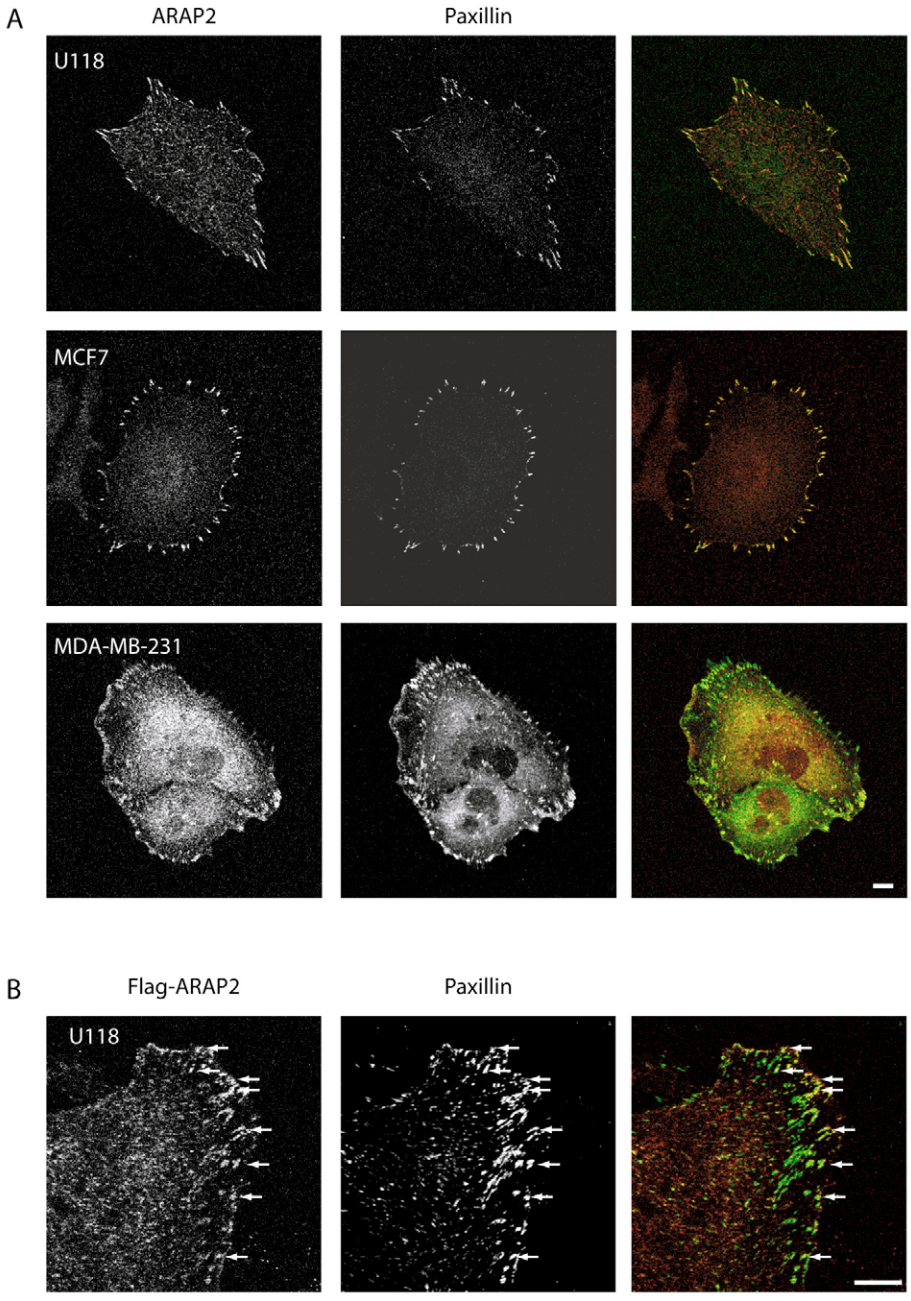


**Fig. 3.** Cellular distribution of ARAP2. (A) Endogenous ARAP2. U118, MCF7 and MDA-MB-231 cells, as indicated, were stained for ARAP2 and paxillin. (B) Epitope-tagged ARAP2. U118 cells expressing Flag-ARAP2 were fixed and stained for the Flag epitope and paxillin. Arrows indicate FAs. Bars, 10 μm.

Materials and Methods for characterization of the antibodies raised). In the cell lines that we examined, including U118 (glioblastoma), MCF7 and MDA-MB-231 (mammary carcinoma) endogenous ARAP2 was at the cell edge and on the ventral surface in linear structures where it colocalized with the focal adhesion components paxillin (Fig. 3A) and vinculin (shown for U118 cells in Fig. 5). When overexpressed, ARAP2 was diffusely distributed throughout the cell; however, at lower expression levels the exogenous protein could be detected at the cell edge and in linear structures with paxillin (Fig. 3B).

Given the association of ARAP2 with FAs, we considered the possibility that ARAP2 affects the formation of these adhesive structures. As an initial test, we examined the effect of changing ARAP2 expression levels on the rate of cell spreading on fibronectin (Fig. 4A). Overexpression of Flag-tagged ARAP2 in U118 glioblastoma cells reduced the rate of spreading. By contrast, cells, in which ARAP2 expression was reduced by transfection with small interference RNA (siRNA), spread more rapidly than the untransfected control cells.

We next determined whether changing expression levels of ARAP2 affected cytoskeleton markers. U118 cells either expressing epitope-tagged ARAP2 or reduced levels of ARAP2 were examined (Fig. 5A). Overexpression of ARAP2 in U118 cells had no detectable effect on the distribution of either vinculin or phosphotyrosine. SFs were present. Paxillin was present in FAs with vinculin but was also diffusely distributed around the nucleus. By contrast, in cells with reduced ARAP2 expression, paxillin, vinculin and phosphotyrosine labeling was reduced and redistributed to the cell edge in structures resembling focal contacts. Moreover,

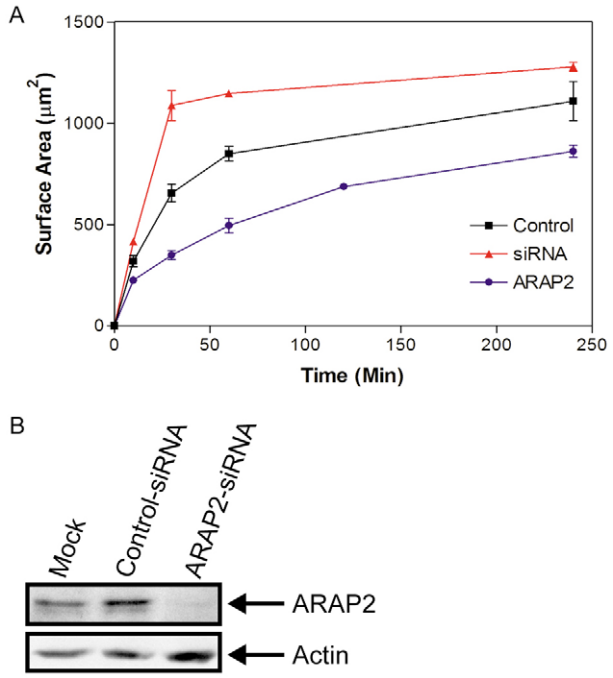


**Fig. 4.** (A) Effect of ARAP2 on cell-spreading rate. U118 cells (control), U118 cells expressing epitope-tagged ARAP2 (ARAP2) or U118 cells treated with siRNA to reduce expression of ARAP2 (siRNA) were trypsinized from plastic flasks, triturated and reseeded on coverslips coated with a solution of 10 μg/ml fibronectin. Cells were fixed at the indicated times and stained for paxillin and either endogenous ARAP2 or Flag epitope. The cells were then examined by confocal microscopy. To quantify the cell spreading at the indicated time, fluorescent images of 50 randomly selected cells were captured using 20× 1.4 NA objectives and surface areas were determined using ImagePro® Plus 5.1 software package. Values are the mean ± standard error of the mean from two independent experiments. (B) Relative ARAP2 levels after siRNA treatment of U118 cells. Cells were either mock-transfected, or transfected with a control siRNA or siRNA targeting ARAP2 as indicated. Three days after transfection, the cells were lysed and analyzed by immunoblotting with specific antibodies to ARAP2.

actin SFs were not observed; instead, actin was concentrated at the cell cortex. Similar results were obtained with MDA-MB-231 and MCF7 cells (not shown). These effects on actin SFs and FAs were also observed when ARAP2 expression was reduced with a different pool of siRNA in the U118 cells (not shown). The effects of siRNA for ARAP2 on actin SFs and FAs could be reversed adding an expression vector for ARAP2 resistant to siRNA (ARAP2 levels, as determined by immunoblotting, are shown in Fig. 5B, effects on cell morphology are shown in Fig. 6A,B).

The role of ArfGAP activity in supporting cytoskeleton changes was determined. First, a point mutant lacking ArfGAP activity, [R728K]ARAP2, was overexpressed in U118 cells. It was found to disrupt SFs and FAs (Fig. 6A,B). Furthermore, it did not reverse the effect of lowering endogenous ARAP2 expression (Fig. 6A,B). We also examined the effect of expressing constitutively active [Q67L]Arf6 in U118 cells. This Arf mutant is effectively 'GTP-locked'. Expression of the mutant could mimic some of the effects of decreasing ARAP2 expression. We found that overexpression of wild-type Arf6 had no detectable effect on SFs but expression of [Q67L]Arf6 resulted in a decrease in SFs similar to that seen with reduction of ARAP2 expression or activity (Fig. 6C). Similar results were obtained with HeLa cells using a fast cycling mutant, [T157A]Arf6 (Santy, 2002), which is also preferentially GTP-bound (not shown).

Formation of SFs also depended on the ability of ARAP2 to bind RhoA-GTP. Overexpression of the point mutant that did not bind RhoA, [K1190P]ARAP2, had no effect on SFs or FAs in cells containing wild-type endogenous ARAP2 and did not rescue the phenotype induced by lowering endogenous ARAP2 expression (Fig. 6A,B). Cells expressing [Q63L]RhoA had robust SFs. By contrast, cells with reduced ARAP2 levels did not have SFs even with the expression of [Q63L]RhoA (Fig. 6D).

### ARAP2 and ROK have differential effects on stress fiber and focal adhesion formation

Rho-kinase (ROKα) has been implicated in the formation of FAs and SFs (Amano et al., 1997; Kimura et al., 1996; Leung et al., 1996). To understand the relationship of the putative effector ARAP2 to this established effector, we expressed ROKα in cells with reduced ARAP2 expression. We found that, although SFs were formed, they were disorganized (Fig. 7A). In addition, the cells did not recover FAs (Fig. 7B). We also expressed constitutively active ROK ([1-478]ROK) in cells treated with siRNA to reduce levels of ARAP2 (Fig. 7C). The cells still formed stellate stress fibers (not shown) but the number of focal adhesions formed (7±1.4 per cell; quantified as described in Materials and Methods) was less than in cells not treated with siRNA (17±4; $P<0.05$) (Fig. 6C). Cells treated with the ROK inhibitor Y27632 (Ishizaki et al., 2000) lacked SFs and FAs (Fig. 7C,D). Increased expression of ARAP2 did not reverse the effect of the drug on these structures (Fig. 7C,D) but did result in the formation of punctate coalescences of paxillin with ARAP2 in 76±3% of the cells (Fig. 7D). We did not detect these paxillin-containing pucta in the control cells treated with Y27632.

## Discussion

The ARAPs are a recently described subset of ArfGAPs that share a common domain organization. Each of the three ARAPs contains an N-terminal SAM domain, an ArfGAP domain, a pair of ankyrin repeats, a RhoGAP domain, an RA domain and five PH domains. Different from ARAP1 and ARAP3, the RhoGAP domain of ARAP2 lacks the catalytic arginine residue characteristic of all other known RhoGAPs and, therefore, was predicted to lack RhoGAP activity. Here, we confirm that ARAP2 indeed lacks RhoGAP activity, but we also found that it binds RhoA-GTP through the RhoGAP domain. Furthermore, ARAP2 expression contributes to the assembly of both SFs and FAs. The function of ARAP2 in this context is dependent on both its interaction with RhoA and its ArfGAP activity, which we found is specific for Arf6.

ARAP1 and ARAP3, which are structurally similar to ARAP2, have previously been found to affect the actin cytoskeleton. ARAP1 is an Arf1/Arf5 GAP in vitro. Consistent with this Arf specificity, ARAP1 is localized to the Golgi complex and overexpression causes redistribution of the Golgi

marker p58 (Miura et al., 2002). ARAP1 also has an active RhoGAP domain. ARAP1 overexpression causes cell rounding and loss of SFs, consistent with a RhoA-specific GAP activity (Miura et al., 2002). ARAP3 is diffusely distributed in cells, with a fraction of the protein associated at the cell periphery and in membrane ruffles (Krugmann et al., 2002; Stacey et al., 2004). Arf specificity has not been unambiguously established (Krugmann et al., 2002; Krugmann et al., 2006; Stacey et al., 2004). Overexpression of ARAP3 causes a loss of SFs in PAE cells, and cell rounding in HEK 293 cells.

ARAP2 is the third ArfGAP found to be associated with FAs, a localization that distinguishes ARAP2 from both ARAP1 and ARAP3. The other two ArfGAPs in FAs are ASAP1, and GIT1 and GIT2 (Turner et al., 2001; de Curtis, 2001; Randazzo and Hirsch, 2004). Each of these ArfGAPs appears to have a different function. ASAP1 and ARAP2

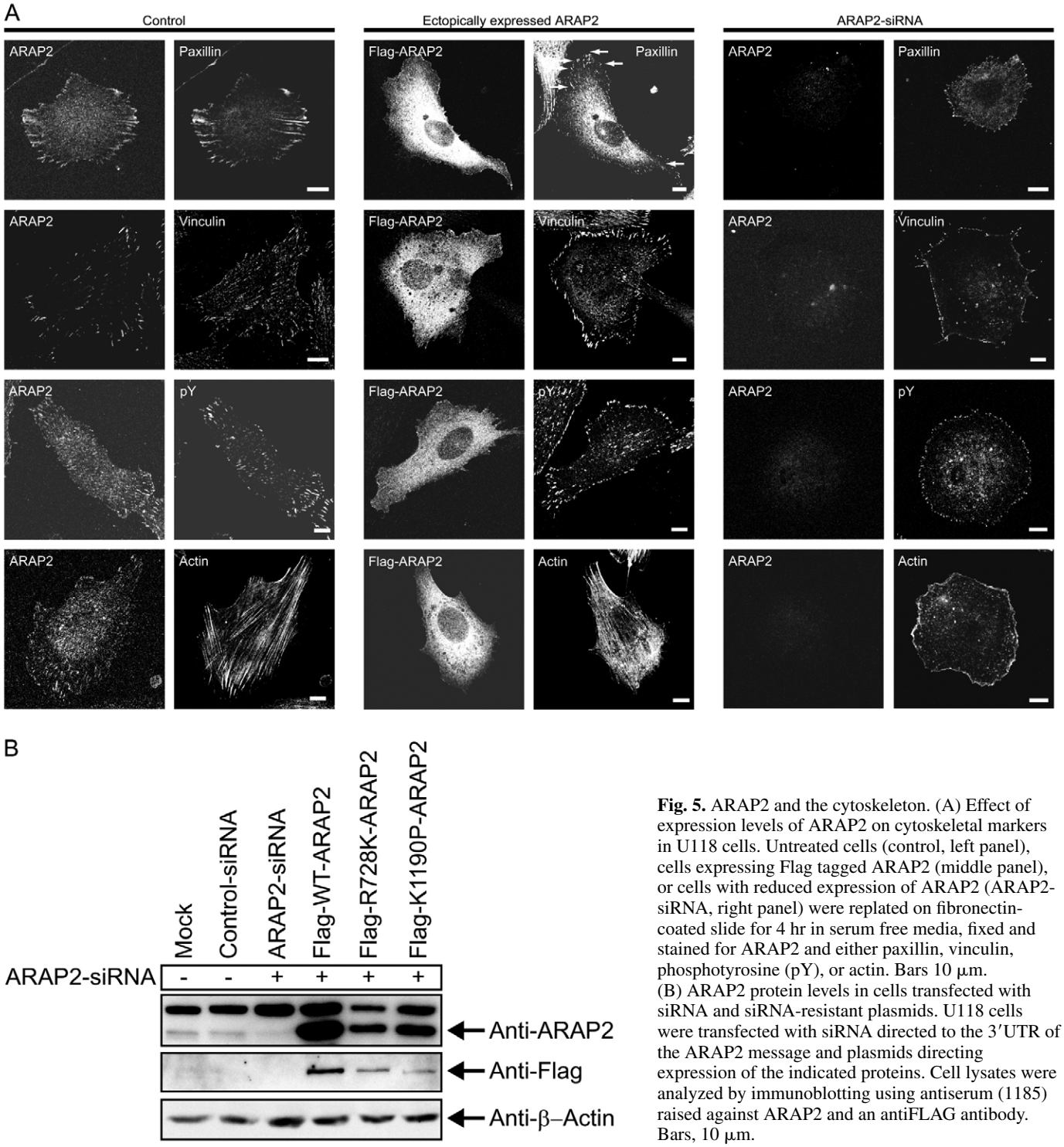


**Fig. 5.** ARAP2 and the cytoskeleton. (A) Effect of expression levels of ARAP2 on cytoskeletal markers in U118 cells. Untreated cells (control, left panel), cells expressing Flag tagged ARAP2 (middle panel), or cells with reduced expression of ARAP2 (ARAP2-siRNA, right panel) were replated on fibronectin-coated slide for 4 hr in serum free media, fixed and stained for ARAP2 and either paxillin, vinculin, phosphotyrosine (pY), or actin. Bars 10 μm. (B) ARAP2 protein levels in cells transfected with siRNA and siRNA-resistant plasmids. U118 cells were transfected with siRNA directed to the 3′UTR of the ARAP2 message and plasmids directing expression of the indicated proteins. Cell lysates were analyzed by immunoblotting using antiserum (1185) raised against ARAP2 and an antiFLAG antibody. Bars, 10 μm.

appear to be antagonists. ASAP1 overexpression causes paxillin to dissociate from FAs and induces the formation of focal complexes (Randazzo et al., 2000b; Liu et al., 2002; Liu et al., 2005). GIT1 and GIT2 appear to function as signaling scaffolds, directly binding both paxillin and the Rac GEF β-PIX (Turner et al., 2001). Given that multiple ArfGAPs with unique Arf specificities associate with FAs, it is likely that multiple Arf proteins function in regulating the dynamics of FAs.

Examination of the Arf specificity of ARAP2 indicated a preference for Arf6 as a substrate. In vitro, Arf6 was a slightly better substrate than Arf5 and was much better than Arf1. In vivo experiments confirmed this substrate specificity: (1) overexpression of ARAP2 induced redistribution of Arf6, but not Arf1 or Arf5; (2) $AlF_4$ induced colocalization of ARAP2 with Arf6 but not Arf1 or Arf5 and; (3) direct measurement of Arf-GTP levels using a GGA3 pull-down assay indicated a preference for Arf6 in vivo.

These results are consistent with the well-established role for Arf6 in cytoskeletal regulation. Arf6 was the first Arf found to be involved in the regulation of actin cytoskeleton dynamics in work examining actin-rich protrusions in HeLa cells (Radhakrishna et al., 1996). Arf6 activity was subsequently found to be necessary for Rac1-dependent plasma membrane ruffling and phagocytosis (Donaldson, 2003; Radhakrishna et al., 1999; Zhang et al., 1998; Palacios and Souza-Schorey, 2003), as well as cell spreading (Song et al., 1998; Dunphy et al., 2006). The inhibitory effect of ARAP2 overexpression on cell spreading is consistent with these previous observations. Particularly relevant to a potential mechanism by which ARAP2 may affect FA formation, Arf6 has been found to influence the trafficking of integrins (Brown et al., 2001; Powelka, 2004; Dunphy et al., 2006).

Our data are consistent with the speculation that ARAP2 functions as a RhoA effector rather than a RhoA GAP. An important difference between ARAP2 and the other ARAPs is that ARAP2 lacks RhoGAP activity. The ability of both ARAP1 and ARAP3 to alter cytoskeletal organization is dependent upon their RhoGAP activity (Krugmann et al., 2002; Miura et al., 2002). We found that ARAP2 does bind RhoA in preference to Cdc42 and Rac, and that binding was mediated by the RhoGAP domain. This result led us to hypothesize that ARAP2 can function as a Rho effector. Consistent with this hypothesis, reduced expression of ARAP2 results in loss of FAs and SFs even in the presence of constitutively active RhoA. Restoration of FAs and SFs required both RhoA-GTP binding and ArfGAP activity.

We also examined how ARAP2 integrates with Rho effectors with an established role in FA formation. The effects of RhoA on the actin cytoskeleton have been thought to rely primarily on actin polymerization and the contraction of actin fibers mediated by mDia, ROKα and PtdIns(4,5)$P_2$ (Watanabe et al., 1999; Ridley, 2001). Among these, ROKα, like ARAP2, affects both SFs and FAs (Watanabe et al., 1999; Ridley, 2001). We found that neither ARAP2 nor ROKα overexpression could completely compensate for the loss of the other protein in the formation of SFs and FAs. ROKα could induce SFs but was inefficient in inducing FAs in cells with reduced ARAP2 expression. Conversely, ARAP2 overexpression did not restore either SFs or FAs formation in cells in which ROK activity was inhibited. However, punctate concentrations of paxillin, absent when cells were treated with the ROK inhibitor, were observed when ARAP2 was overexpressed.

How do ARAP2 and its substrate Arf6 function to control FA and SF assembly? We speculate that Arf6 controls the trafficking of integrins into and/or out of FAs. Results of recent work examining Arf6 and the Arf6-specific GEF BRAG2 are consistent with a role for Arf6 in integrin endocytosis and recycling (Dunphy et al., 2006). Thus, RhoA, by binding to ARAP2, could regulate Arf6-dependent trafficking of FA proteins including integrins with targeting to a restricted membrane locus. The resulting concentration of FA elements could serve as a nidus to drive the formation of FAs. Actin polymerization and tension on the resulting SFs contribute to these events, but could be independently regulated by mDia and ROKα. Such a model does not exclude additional coordinating mechanisms for actin polymerization and FA formation including, for instance, phosphorylation of ARAP2 by ROKα.

In summary, we report that ARAP2 mediates RhoA effects on SFs and FAs in a manner that is strictly dependent on its activity as an Arf6-specific GAP. We speculate that ARAP2 affects the trafficking and/or organization of FA component proteins. However, additional work is needed to define the role of Arf6 in this context.

## Materials and Methods

### Plasmids

Expression vectors for full-length ARAP2, [467-930]ARAP2, [1114-1433]ARAP2, [875-1704]ARAP2 and [1317-1433]ARAP2 with a Flag epitope (DYKDDDDK) fused to the N-terminus were generated by PCR amplification of the appropriate reading frame. The PCR product was ligated into the pCI vector (Promega, Madison, WI). Point mutations in the ArfGAP domain (R728K) and RhoGAP domain (K1190P) regions were obtained by site-directed mutagenesis with the Quickchange® II XL kit (Stratagene, La Jolla, CA). pGEX-3X-rhotekin RBD plasmid, pGEX-3X-PAK RBD plasmid and mammalian expression vectors for ROKα-HA, GFP[1-478]ROKα, [Q63L]RhoA-AU5, RhoA-AU5, Cdc42-AU5 and Rac1-AU5 were generous gifts from Silvio Gutkind (National Institutes of Health) and an expression vector for p190RhoGAP was a generous gift from Sarah Parsons (University of Virginia at Charlottesville, VI). Bacterial expression vectors for His-Cdc42, His-RhoA and His-Rac1 were generous gifts from Yi Zheng (Childrens Hospital, Cincinatti, Ohio). A plasmid for the expression of VHS-GAT of GGA3 fused to GST has been described (Puertollano et al., 2001; Santy and Casanova, 2001).

### Antibodies and reagents

Rabbit anti-ARAP2 antisera were raised against the synthetic peptides RSRTLPKELQDEQILK, residues 1689-1704 of ARAP2 (antisera 1185), and ANVHKTKKNDDPSKDY, residues 78-93 of ARAP2 (antisera 1187), conjugated by an N-terminal cysteine to maleimide-activated KLH (Pierce Biotechnology, Inc., Rockford, IL) at Covance Research (Princeton, NJ). The antisera recognized recombinant ARAP2. The results using antiserum raised to residues 1689-1704 of ARAP2 is shown (positive control, Fig. 8A). A protein with a molecular mass of ~190 kDa co migrating with recombinant ARAP2 was detected by immunoblotting in lysates from five of seven cell lines examined (Fig. 8A). The signal was blocked by incubating the serum with the peptide to which the antibody was raised; however, the antiserum yielded a signal at ~250 kDa that was also blocked by the peptide. We therefore treated two cell lines with siRNA targeting ARAP2 to obtain further evidence that the band detected at 190 kDa was endogenous ARAP2. In both cases, only the band at ~190 kDa was diminished (Fig. 8B). We also tested the antiserum for suitability in immunofluorescence microscopy. A fluorescent signal was obtained at the cell edge and in linear structures behind the cell edge that colocalized with paxillin (Fig. 8C). This signal was blocked with the peptide to which the antiserum was raised. More importantly, the immunofluorescence (IF) signal was greatly diminished by siRNA treatment indicating that the primary protein recognized by IF was the 190-kDa species seen by immunoblotting. To further test whether the signal observed in focal adhesions was from ARAP2, both antisera (1185 and 1187) were affinity-purified using the peptides against which the antibodies were raised with a purification kit from Pierce (Rockford, IL). Although affinity purification of 1185 did not remove the signal at 250 kDa, both affinity purified antisera, 1185 and 1187, recognized a band at 190 kD by immunoblotting (Fig. 8C). In addition, colocalization of a signal with paxillin was observed when

either affinity purified antibody was used for immunoblotting (Fig. 8D). Taken together, these results are consistent with ARAP2 localizing with FAs and also indicate that either antibody was suitable for following ARAP2 in these structures.

Monoclonal M5 anti-FLAG epitope Ab, M2 anti-FLAG affinity matrix, monoclonal anti-Vinculin Ab were purchased from Sigma-Aldrich (St Louis, MO). Monoclonal anti-hemagglutinin (HA) Ab was from Roche Molecular Biochemicals (Indianapolis, IN) and polyclonal anti-FLAG Ab was from Rockland Immunochemicals (Gilbertsville, PA). Polyclonal anti-AU5 and anti-HA Abs were obtained from Covance. Rhodamine-conjugated phalloidin was purchased from Molecular Probes (Carlsbad, CA). Monoclonal anti-Paxillin Ab was from BD Biosciences, Transduction Laboratories (Franklin Lakes, NJ), anti-phosphotyrosine (4G10) was from Upstate Biotechnology (Lake Placid, NY), Fluorescein- or Texas Red-conjugated secondary Abs were purchased form Jackson Immunoresearch (West Grove, PA). Horseradish-peroxidase-conjugated anti-mouse IgG and anti-rabbit IgG were from Bio-Rad Laboratories (Hercules, CA). Phosphatidic acid and PtdIns(4,5)$P_2$ were from Sigma-Aldrich. Phosphatidylinositol (3)-phosphate [PtdIns(3)*P*] was from Biomol (Plymouth Meeting, PA). PtdIns(3,4,5)$P_3$, phosphatidylinositol (3,5)-bisphosphate [PtdIns(3,5)$P_2$], and phosphatidylinositol 3,4-bisphosphate [PtdIns(3,4)$P_2$] were purchased from Calbiochem (San Diego, CA).

## Cell culture and transfection

Cells were maintained in Dulbecco's modified Eagle's medium (DMEM) with 10% fetal bovine serum, 100 U/ml penicillin, and 100 μg/ml streptomycin (Invitrogen, Carlsbad, CA) at 37°C with 5% $CO_2$. Cell transfection was performed using FuGENE6 reagent in accordance with the manufacturer's instructions for plasmid DNA (Roche). For RNAi assays, 19-nucleotide siRNA duplexes with 3′-UU overhangs specific for the 3′-untranslated region (3′-UTR) (5′-GUAAGAAG-ACAUUGGGUUAUU-3′) and the open reading frame (ORF) (SmartPool) of human ARAP2 (GenBank accession number NM_015230) were purchased from Dharmacon Inc. (Lafayette, CO). The siRNA targeting the UTR was used for all experiment shown. Use of this particular RNA allowed rescue using plasmids

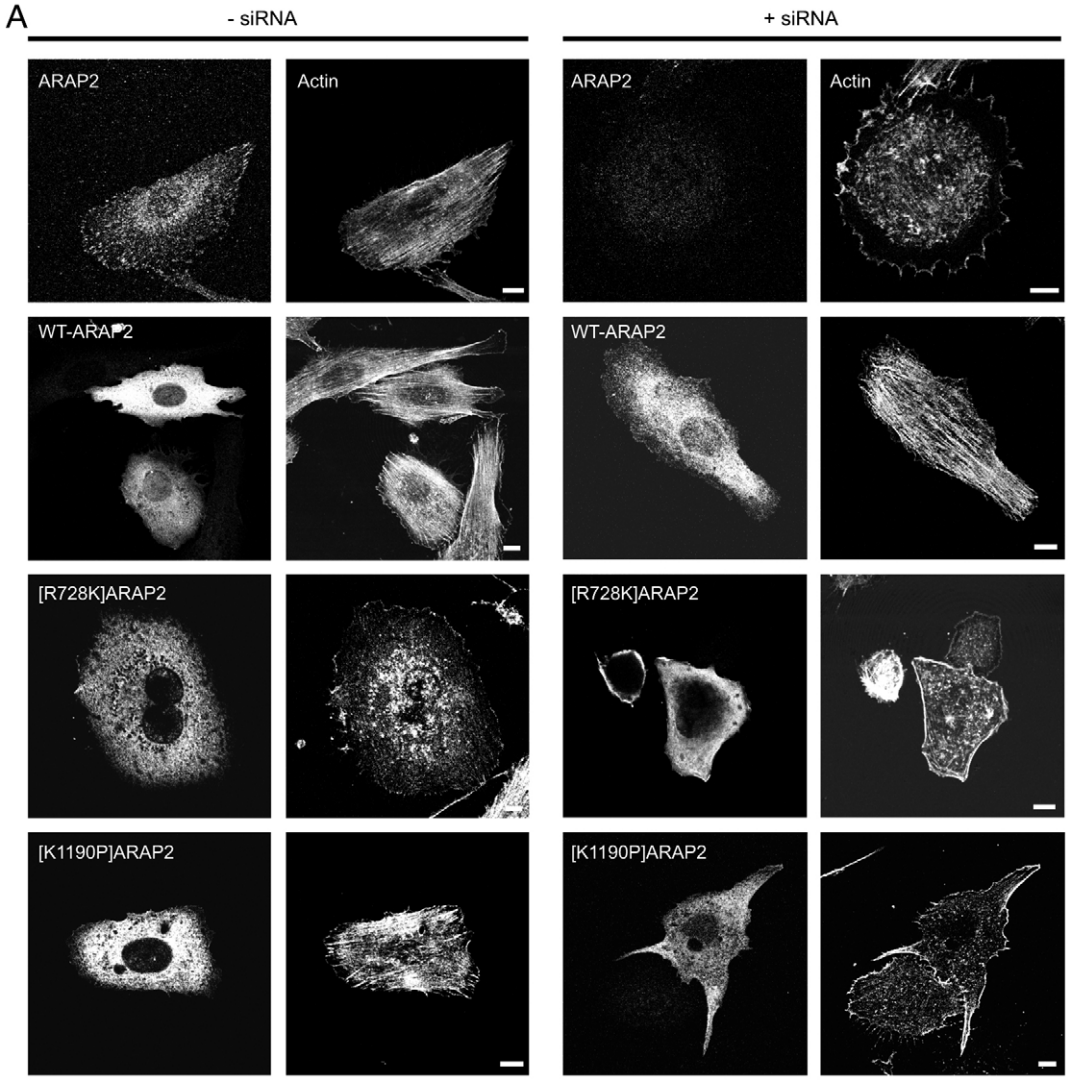


**Fig. 6.** ARAP2 and the cytoskeleton. (A,B) Role of ArfGAP and RhoGAP domains in effects of ARAP2 on cytoskeleton. Effect of replacing endogenous ARAP2 with recombinant ARAP2 on stress fiber (A) and focal adhesion (B) formation. U118 cells were transfected with empty vector, Flag-ARAP2, Flag-[R728K]ARAP2, or Flag-[K1190]ARAP2 with (right panel) or without (left panel) ARAP2 siRNA. Three days after transfection, cells were seeded onto fibronectin-coated slides, fixed, and stained with polyclonal anti-ARAP2 Ab and either Rhodamine-phalloidin to visualize actin (A) or monoclonal anti-paxillin Ab to visualize focal adhesions (B). (C) Effect of [Q67L]Arf6 on stress fibers in U118 cells. Cells were transfected with either plasmids for the expression of wild type or [Q67L]Arf6-HA. After 24 hours the cells were replated on fibronectin-coated coverslips, incubated for 6 hours in serum-free medium and then stained for epitope-tagged Arf6 and actin. (D) Effect of ARAP2 expression level on stress fibers induced by [Q63L]RhoA. Cells were co-transfected with siRNA targeting ARAP2 and an expression plasmid for [Q63L]RhoA, fixed and stained for RhoA and polymerized actin. Bars, 10 μm.

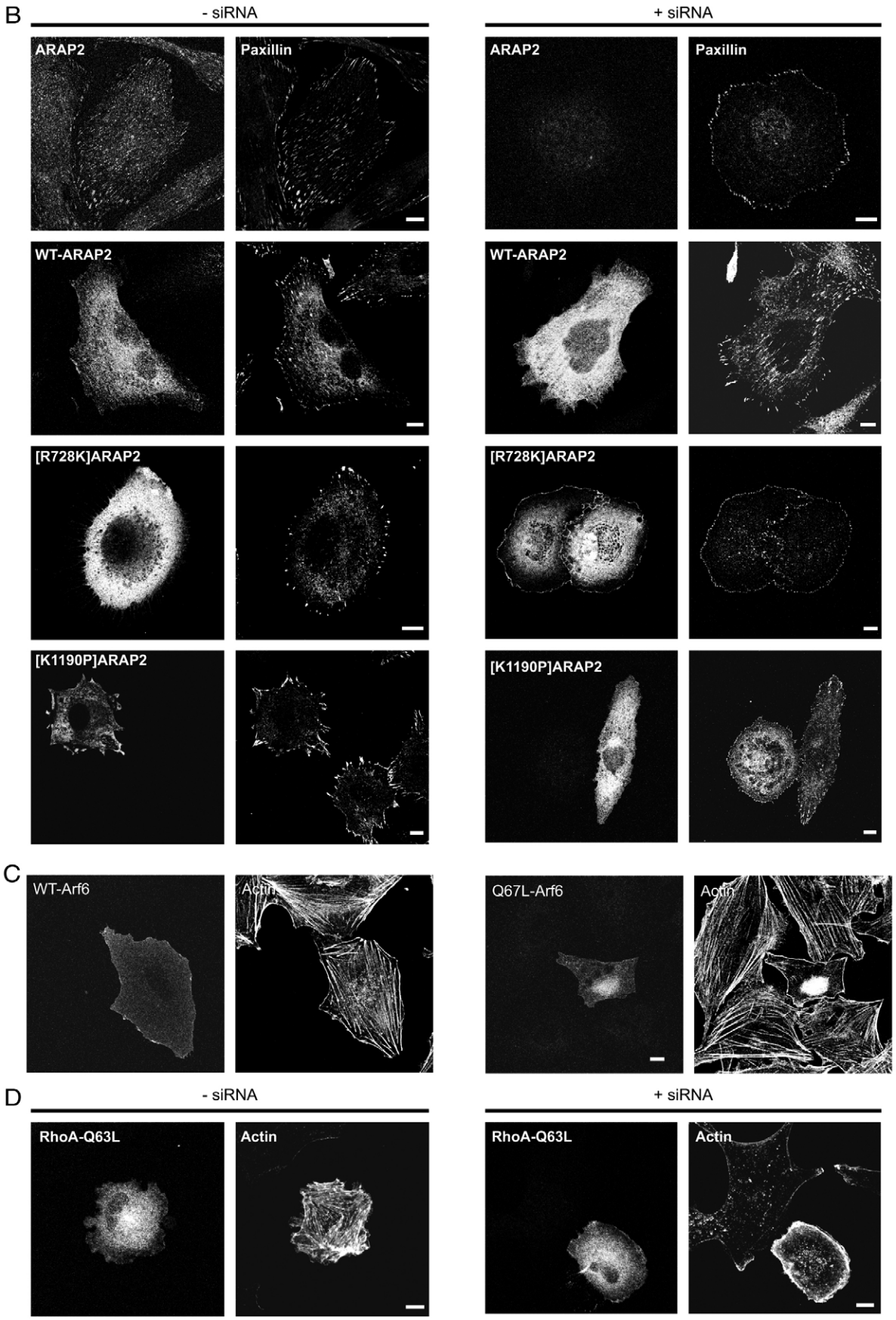


**Fig. 6.** See previous page for legend.

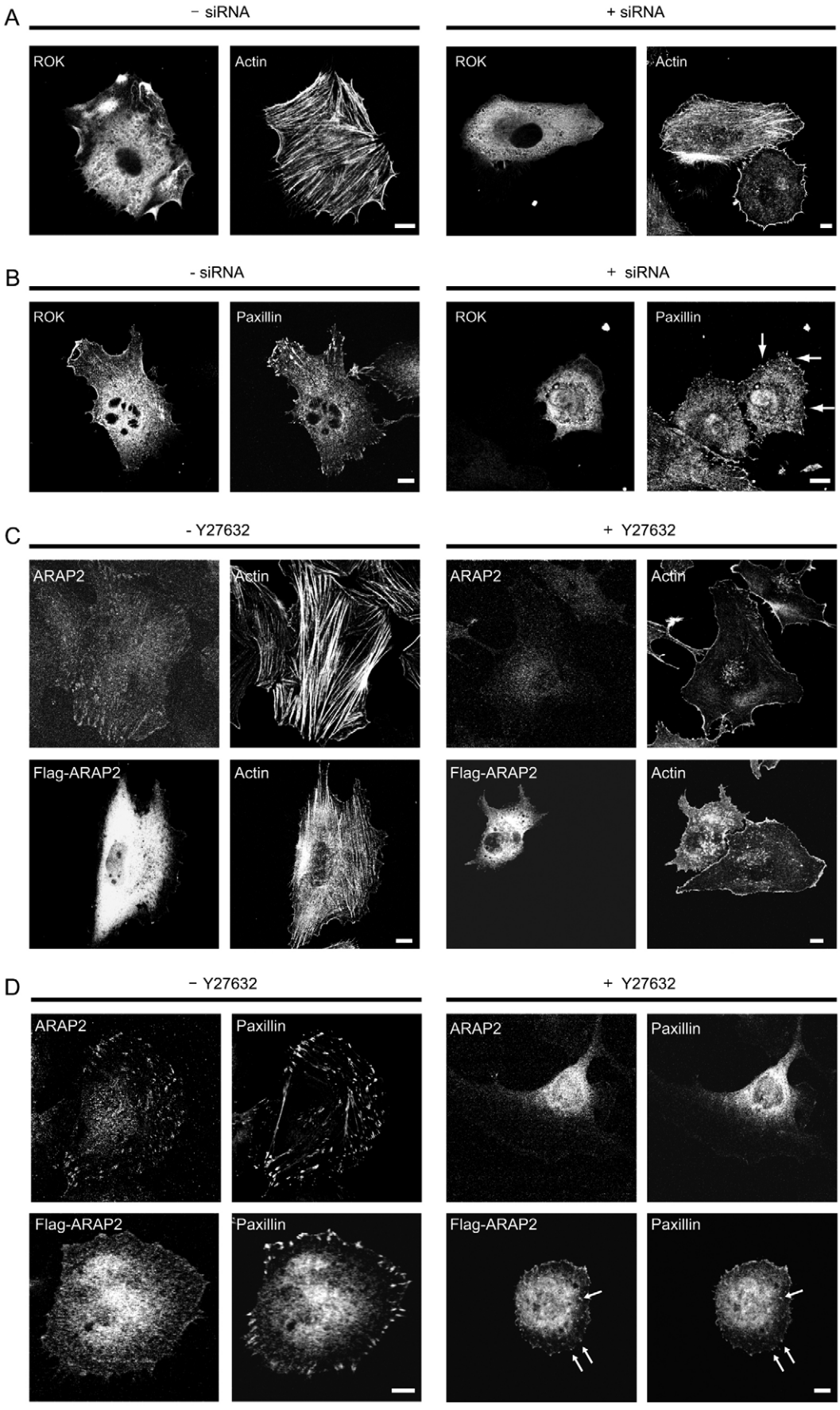


**Fig. 7.** Relationship of ROKα and ARAP2. (A,B) Effect of ROKα on cells with reduced ARAP2 expression. U118 cells were transfected with a plasmid for expression of HA tagged-ROKα and ARAP2-siRNA (right panels) and stained using polyclonal anti-HA and either Rhodamine-phalloidin for actin (A) or a monoclonal Ab for paxillin (B). (C) Effect of activated ROK on FA formation in cells with reduced ARAP2 levels. The experiment was similar to that described in B but using GFP-[1-478]ROK instead of full-length ROK. (D,E) Effect of ARAP2 on cells with inhibited ROK activity. U118 cells were transfected with a plasmid for the expression of ARAP2. Twenty-four hours later, the cells were treated with Y27632, a specific ROK inhibitor. The cells were fixed and stained for ARAP2 and either actin (C) or paxillin (D) as indicated. Arrows point to focal contacts. Bars, 10 μm.

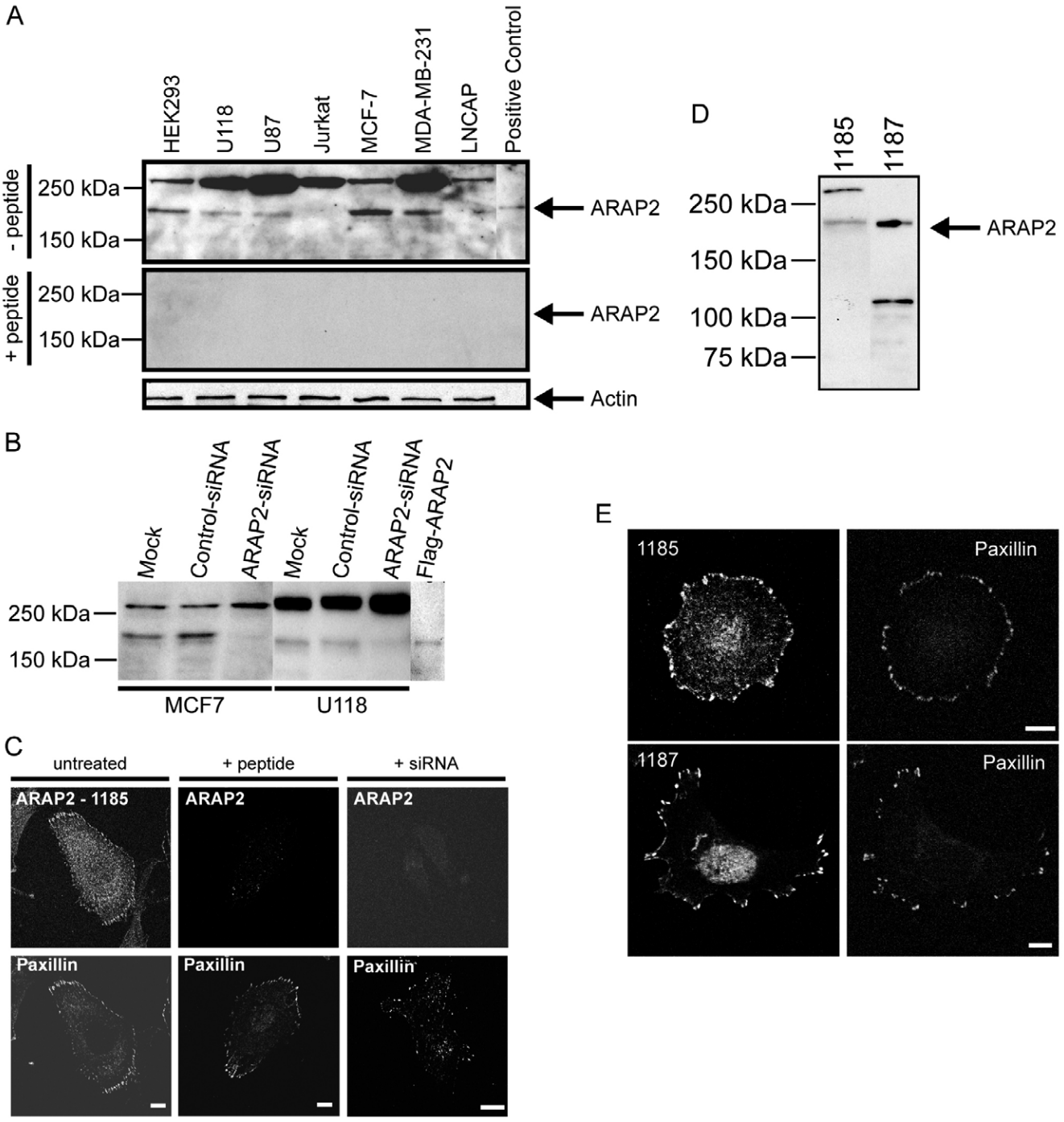


**Fig. 8.** Characterization of antibody for ARAP2. (A) ARAP2 protein levels in cultured cells. ARAP2 was detected by western blotting using antibody 1185, which was raised against amino acid residues 1689-1704 of ARAP2 as described in Materials and Methods. HEK 293, human embryonic kidney 293 cells; U118, glioblastoma cells; U87, glioblastoma cells; Jurkat, T lymphocyte cells; MCF-7, breast adenocarcinoma cells; MDA-MB-231, advanced breast adenocarcinoma cells; LNCAP, prostate cancer cells. A lysate from cells transiently transfected with a plasmid directing expression of Flag-ARAP2 was used a positive control. Actin was used as a control for normalization. In the middle panel, the signal was blocked by incubating the antibody with the peptide (10 μg/ml) against which the antibody was raised. (B) Effect of siRNA treatment of cells on proteins detected by antiserum 1185. The indicated cell lines were treated for 72 hours with a irrelevant siRNA (control siRNA) or siRNA targeting the 3′UTR of ARAP2 and then lysed for immunoblotting. (C) Characterization of antiserum 1185 against ARAP2 in immunofluorescence. The effect of peptide treatment of antibody and siRNA treatment of cells was examined in the indicated panels. The cells were counterstained for paxillin. Note that the signal for paxillin is easily detected on siRNA treatment but is also altered by the siRNA as described in the article. (D) Antibodies affinity-purified from 1185 and 1187 antisera. Rabbit anti-ARAP2 antisera raised against the synthetic peptides RSRTLPKELQDEQILK, residues 1689-1704 of ARAP2 (antiserum 1185), and ANVHKTKKNDDPSKDY, residues 78-93 of ARAP2 (antiserum 1187) were affinity-purified and used for immunoblotting of lysates from MCF7. (E) Immunofluorescence with affinity purified antibodies. Immunofluorescence of MCF7 cells was performed as in (C) but with affinity-purifed antibodes from antisera 1185 and 1187.

containing the open reading frame. Experiments confirming the effect of ARAP2 expression reduction on SFs and FAs were also performed with siRNA targeting the ORF. A scrambled siRNA was used as a negative control (siCONTROL non-targeting siRNA no. 1, Dharmacon). For transfection, U118 glioma cells were seeded in six-well plates and allowed to reach 40% confluence. After 24 hours, cells were transfected with 100 nM siRNA with Oligofectamine (Invitrogen) according to the manufacturer's instructions. Transfection was done in the absence of fetal bovine serum (FBS), which was replenished 4 hours after each transfection. Mock transfections were performed in an identical manner to siRNA transfections, except that siRNA was omitted. For rescue assays, U118 cells were first transfected with WT ARAP2, [R728K]ARAP2 or [K1190P]ARAP2 by incubating with a mixture of 4 μg DNA and 12 μl FuGENE6 reagent in the absence of FBS. After 2 hours, the cells were transfected with siRNA and, 4 hours later, the transfection medium was replenished with fresh medium containing FBS.

### Immunoprecipitaion and immunoblotting

Transfected cells were harvested after 24- to 48-hour transfection, washed and lysed with 25 mM Tris pH 8.0, 25 mM NaCl, 1% Triton X-100, 10% glycerol and Complete™ protease inhibitor cocktail (Roche). The cell lysates were cleared by centrifugation at 10,000 ***g*** for 10 minutes at 4°C and incubated with anti-FLAG M2 gel (Sigma-Aldrich) overnight at 4°C. The beads were washed three times with lysis buffer and eluted with SDS-PAGE sample buffer and the bound proteins were analyzed by western blot with specific Abs and detected by SuperSignal® West Dura Extended Duration Substrate (Pierce).

### Purification of recombinant proteins

N-terminal Flag-tagged WT ARAP2 and [467-930]ARAP2 were overexpressed in HEK 293 cells by transient transfection. The cells were lysed and the overexpressed protein was immunoprecipitated with M2 anti-FLAG agarose affinity gel and eluted with Flag peptide (400 μg/ml, Sigma-Aldrich). The eluted proteins were further purified through PIP Beads™ di-C6 PI(3,4,5)P3 phosphoinositide-coated agarose beads (Echelon, Salt Lake City, Utah). His-tagged proteins expressed in bacteria were purified by batch chromatography on Ni-chelate resin by standard methods.

### Determination of nucleotide-dependent RhoA-ARAP2 binding

GST and GST-RhoA, expressed in BL21 cells, were extracted and purified on glutathione-Sepharose 4B gel (Amersham Bioscience, Piscataway, NJ). The immobilized GST fusion proteins were incubated for 30 minutes with the indicated nucleotide with lysates of cells expressing the indicated recombinant ARAP2 proteins. The beads were chilled, collected by centrifugation and washed three times with ice-cold lysis buffer. Proteins were eluted from the beads by boiling in SDS-PAGE sample buffer and detected by immunoblotting using the polyclonal anti-FLAG Ab.

### Determination of in vivo RhoA-GTP, Rac1-GTP, Cdc42-GTP and Arf-GTP levels

RhoA-GTP, Rac1-GTP and Cdc42-GTP levels in HEK 293 cells transiently expressing RhoA-AU5, Rac1-AU5, or Cdc42-AU5 with ARAP2 or p190RhoGAP were determined using GST fusion protein containing the RhoA-binding domain of Rhotekin or GST fusion protein containing the Rac1- and/or Cdc42-binding domain of PAK to capture the Rho family proteins complexed with GTP as described (Ren et al., 1999). Arf•GTP was determined as described (Santy and Casanova, 2001; Yoon et al., 2005) in a similar way using GST-VHS-GAT$_{GGA3}$ to capture Arf-GTP. Expression of recombinant p190RhoGAP, ARAP2, ASAP1 and ACAP1 was determined by immunoblotting samples of the cell lysates with polyclonal anti-FLAG Ab for ARAP2, ASAP1 and ACAP1 or polyclonal anti-HA for p190RhoGAP.

### Immunofluorescence staining

Cultured cells were reseeded on fibronectin-coated coversplips for 4 hours and fixed using 2% formaldehyde in phosphate-buffered saline (PBS) and processed for immunofluorescence as described (Miura et al., 2002). The cells were examined by confocal microscopy with a Zeiss Axiovert 200 M inverted microscope with a Zeiss LSM 510 NLO confocal system (Carl Zeiss MicroImaging, Thornweed, NY) operated at room temperature with fixed cells and a Plan-Apochromat oil immersion objective. Zeiss AIM software was used to sequentially collect FITC and Rhodamine signals with a BP 500-550 nm filter and a BP 565-615 nm filter after sequential excitation with the 488 nm and 543 nm laser lines. Adobe Illustrator was used to prepare the images for publication. Focal adhesions were quantified using Image-Pro Ver 5.12 (MediaCybernetics, MD). For this analysis, random images for each experimental group were collected with identical microscope settings. A typical focal adhesion was used to set threshold intensities for evaluating all images. Objects with a greater intensity than the threshold and an area greater than 1 $\mu m^2$ were counted as focal adhesions.

### Determination of cell spreading

U118 glioma cells transfected with a scrambled siRNA, ARAP2-targeted siRNA or an expression vector for recombinant ARAP2 were reseeded on fibronectin-coated slides, incubated for 10, 30, 60 and 240 minutes and fixed. To quantify the cell spreading, fluorescent images of 50 randomly selected cells were captured using 20×1.4 NA objectives and surface areas were determined using Image-Pro® Plus 5.1 software package (Media Cybernetics, LP).

### Modeling and analysis of the RhoGAP domain structure

Computational studies were performed on a Silicon Graphics Octane 2 workstation, equipped with dual 360 MHz R12000 processors. The sequence of ARAP2 with primary accession number Q8WZ64 was obtained from GenBank. Only the mature sequences starting from residues 1116-1297 Rho-GAP domain were considered in deriving the homology model. A WUBLAST 2.0 (blast.wustl.edu/) search and the Unity module of Sybyl 6.9 (Tripos Associates Inc., St Louis, MO) were performed on the sequence. The Psipred protein structure prediction server was utilized for the secondary structure prediction (Godzik et al., 1992; McGuffin et al., 2000). The crystal structure from p50rhoGAP starting from residues 234 to 431 (PDB ID:1AM4) with primary accession number Q07960 was chosen to build the human ARAP2 model structure. The sequence identity of templates with target was 27.43%. Comparative protein modeling was performed with the Composer module of Sybyl 6.9 (Tripos Assoc. Inc, St Louis MO). Energy minimizations and molecular dynamics were accomplished in the Discover module of InsightII 2000 (Accelrys Inc., San Diego, CA). The geometrical and local environmental consistencies of the model were evaluated with ProStat and Profiles-3D (Luthy et al., 1992) modules of InsightII 2000 and the MatchMaker module of Sybyl 6.9. The alignment and identification of the structurally conserved regions (SCRs) and structurally variable regions (SVRs) was carried out as described (Sabnis et al., 2003). Coordinates for the SCRs were assigned from the template molecule. The coordinates of SVRs were obtained using the conformational search program GeneFold and MatchMaker modules in Sybyl 6.9. SVR loop regions were built using the protein loop search protocol (Jones and Thirup, 1986) as available in Composer. The model obtained was then refined by minimization using a similar protocol as described earlier (Sabnis et al., 2003). The final total energy was –5125.146 kJ/mole. Minor adjustments of the human ARAP2 sequence alignment were made to ensure correct positioning of all conserved residues. Appropriate loop models were selected on the basis of acceptable stereochemical parameters (allowable phi and psi angles on a Ramachandran plot). The solvation model was used to implicitly introduce the effect of solvent (Stouten et al., 1993). In the first stage, the Monte Carlo minimization method was used using random combinations of translational and rotational motions each followed by 2500 iterations of conjugate gradient minimization. During this stage a purely repulsive bonded quartic potential was used for modeling the van der Waals interactions while the coulombic interactions were set to zero. In the second stage, the structure was then subjected to molecular dynamics simulation for 5000 iterations of equilibration at 300K. The non-bonded interactions were calculated using a more refined cell-multipole method (Greengard and Rokhlin, 1987) with a distance dependent dielectric constant. Newton's equations of motion were integrated using the Verlet algorithm (Verlet, 1967) with a time step of 1 fsecond using NVT ensemble. Temperature was controlled via direct scaling of the atom velocity motion. Finally, the structures were judged complete when gradient steps of 0.001 kcal/mol/Å or less were reached in conjugate gradient minimization. Further validation of the structures is provided by analysis of the stereochemistry of the structure with the programs Procheck (Laskowski et al., 1992). The visualization of spatial surface was performed through Connolly's program (designated as Connolly surfaces). All the figures were generated by the Pymol (www.pymol.org) program.

### Miscellaneous

Statistical analyses were performed using GraphPad Prism for Windows version 4.0 (GraphPad, www.graphpad.com). RhoGAP activity was determined as described previously (Miura et al., 2002) with the exception that purified His-tagged (rather than GST-tagged) Rho-family proteins were used. ArfGAP activity was determined as described (Che et al., 2006) in a reaction containing 25 mM HEPES (pH 7.4), 100 mM NaCl, 1 mM GTP, 2 mM $MgCl_2$, 1 mM dithiothreitol, Arf-[α-$^{32}$P]GTP, and lipid micelles consisting of 50 μM phosphatidic acid, 10 μM PtdIns(3,4)$P_2$, and 100 nM PtdIns(3,4,5)$P_3$ with 0.1% (v/v) Triton X-100.

We thank Sarah Parsons for the plasmid for mammalian expression of p190RhoGAP, J. Thomas Parsons and Martin Schwartz (all University of Virginia, Charlottesville, VA) for advice and Katherine Stanley for technical assistance. We also thank Stephen Wincovitch and Susan Garfield (Center for Cancer Research, NCI) for assistance in confocal microscopy, particularly in the quantitation of signals. This research was supported by the Intramural Research Program of the NIH, Center for Cancer Research, National Cancer Institute (P.R.) and National Institute of Arthritis and Musculoskeletal and Skin Diseases (B.A.) and NIH grant GM 662510 (J.E.C.).

## References


**Amano, M., Chihara, K., Kimura, K., Fukata, Y., Nakamura, N., Matsuura, Y. and Kaibuchi, K.** (1997). Formation of actin stress fibers and focal adhesions enhanced by Rho-kinase. *Science* **275**, 1308-1311.

**Brown, F. D., Rozelle, A. L., Yin, H. L., Balla, T. and Donaldson, J. G.** (2001). Phosphatidylinositol 4,5-bisphosphate and Arf6-regulated membrane traffic. *J. Cell Biol.* **154**, 1007-1017.

**Brown, M. T., Andrade, J., Radhakrishna, H., Donaldson, J. G., Cooper, J. A. and Randazzo, P. A.** (1998). ASAP1, a phospholipid-dependent Arf GTPase-activating protein that associates with and is phosphorylated by Src. *Mol. Cell. Biol.* **18**, 7038-7051.

**Che, M. M., Nie, Z. and Randazzo, P. A.** (2006). Assays and properties of the Arf GAPS AGAP1, ASAP1 and Arf GAP1. *Methods Enzymol.* **404**, 147-163.

**de Curtis, I.** (2001). Cell migration: GAPs between membrane traffic and the cytoskeleton. *EMBO Rep.* **2**, 277-281.

**Demali, K. A., Wennerberg, K. and Burridge, K.** (2003). Integrin signaling to the actin cytoskeleton. *Curr. Opin. Cell Biol.* **15**, 572-582.

**Donaldson, J. G.** (2003). Multiple roles for Arf6: sorting, structuring, and signaling at the plasma membrane. *J. Biol. Chem.* **278**, 41573-41576.

**Donaldson, J. G. and Jackson, C. L.** (2000). Regulators and effectors of the ARF GTPases. *Curr. Opin. Cell Biol.* **12**, 475-482.

**Dunphy, J. L., Moravec, R., Ly, K., Lasell, T. K. and Casanova, J. E.** (2006). The Arf6 GEF GEP100/BRAG2 regulates cell adhesion by controlling endocytosis of β1 integrins. *Curr. Biol.* **16**, 315-320.

**Faucherre, A., Desbois, P., Satre, V., Lunardi, J., Dorseuil, O. and Gacon, G.** (2003). Lowe syndrome protein OCRL1 interacts with Rac GTPase in the trans-Golgi network. *Hum. Mol. Genet.* **12**, 2449-2456.

**Fukata, Y., Amano, M. and Kaibuchi, K.** (2001). Rho-Rho-kinase pathway in smooth muscle contraction and cytoskeletal reorganization of non-muscle cells. *Trends Pharmacol. Sci.* **22**, 32-39.

**Furman, C., Short, S. M., Subramanian, R. R., Zetter, B. R. and Roberts, T. M.** (2002). DEF-1/ASAP1 is a GTPase-activating protein (GAP) for ARF1 that enhances cell motility through a GAP-dependent mechanism. *J. Biol. Chem.* **277**, 7962-7969.

**Geho, D. H., Bandle, R. W., Clair, T. and Liotta, L. A.** (2005). Physiological mechanisms of tumor-cell invasion and migration. *Physiology* **20**, 194-200.

**Godzik, A., Kolinski, A. and Skolnick, J.** (1992). Topology fingerprint approach to the inverse protein folding problem. *J. Mol. Biol.* **227**, 227-238.

**Greengard, L. and Rokhlin, V. I.** (1987). A fast algorithm for particle simulations. *J. Comp. Phys.* **73**, 325-348.

**Hall, A.** (1998). Rho GTPases and the actin cytoskeleton. *Science* **279**, 509-514.

**Ishizaki, T., Uehata, M., Tamechika, I., Keel, J., Nonomura, K., Maekawa, M. and Narumiya, S.** (2000). Pharmacological properties of Y-27632, a specific inhibitor of Rho-associated kinases. *Mol. Pharm.* **57**, 976-983.

**Jackson, T. R., Brown, F. D., Nie, Z. Z., Miura, K., Foroni, L., Sun, J. L., Hsu, V. W., Donaldson, J. G. and Randazzo, P. A.** (2000). ACAPs are Arf6 GTPase-activating proteins that function in the cell periphery. *J. Cell Biol.* **151**, 627-638.

**Jones, T. A. and Thirup, S.** (1986). Using known substructures in protein model building and crystallography. *EMBO J.* **5**, 819-822.

**Kimura, K., Ito, M., Amano, M., Chihara, K., Fukata, Y., Nakafuku, M., Yamamori, B., Feng, J. H., Nakano, T., Okawa, K. et al.** (1996). Regulation of myosin phosphatase by Rho and Rho-Associated kinase (Rho-kinase). *Science* **273**, 245-248.

**Klein, S., Franco, M., Chardin, P. and Luton, F.** (2005). AlFx affects the formation of focal complexes by stabilizing the Arf-GAP ASAP1 in a complex with Arf1. *FEBS Lett.* **579**, 5741-5745.

**Krugmann, S., Anderson, K. E., Ridley, S. H., Risso, N., McGregor, A., Coadwell, J., Davidson, K., Eguinoa, A., Ellson, C. D., Lipp, P. et al.** (2002). Identification of ARAP3, a novel PI3K effector regulating both Arf and Rho GTPases, by selective capture on phosphoinositide affinity matrices. *Mol. Cell* **9**, 95-108.

**Krugmann, S., Andrews, A., Stephens, L. and Hawkins, P. T.** (2006). ARAP3 is essential for formation of lamellipodia after growth factor stimulation. *J. Cell. Sci.* **119**, 425-432.

**Laskowski, R. A., MacArthur, M. W., Moss, D. S. and Thornton, J. M.** (1992). PROCHECK: a program to check the stereochemical quality of protein structures. *J. Appl. Cryst.* **26**, 283-291.

**Leung, T., Chen, X. Q., Manser, E. and Lim, L.** (1996). The p160 RhoA-binding kinase ROK alpha is a member of a kinase family and is involved in the reorganization of the cytoskeleton. *Mol. Cell. Biol.* **16**, 5313-5327.

**Liu, Y. H., Loijens, J. C., Martin, K. H., Karginov, A. V. and Parsons, J. T.** (2002). The association of ASAP1, an ADP ribosylation factor-GTPase activating protein, with focal adhesion kinase contributes to the process of focal adhesion assembly. *Mol. Biol. Cell* **13**, 2147-2156.

**Liu, Y., Yerushalmi, G. M., Grigera, P. R. and Parsons, J. T.** (2005). Mislocalization or reduced expression of Arf GTPase-activating protein ASAP1 inhibits cell spreading and migration by influencing Arf1 GTPase cycling. *J. Biol. Chem.* **280**, 8884-8892.

**Luthy, R., Bowie, J. U. and Eisenberg, D.** (1992). Assessment of protein models with three-dimensional profiles. *Nature* **356**, 83-85.

**Maekawa, M., Ishizaki, T., Boku, S., Watanabe, N., Fujita, A., Iwamatsu, A., Obinata, T., Ohashi, K., Mizuno, K. and Narumiya, S.** (1999). Signaling from Rho to the actin cytoskeleton through protein kinases ROCK and LIM-kinase. *Science* **285**, 895-898.

**McGuffin, L. J., Bryson, K. and Jones, D. T.** (2000). The PSIPRED protein structure prediction server. *Bioinformatics* **16**, 404-405.

**Miura, K., Jacques, K. M., Stauffer, S., Kubosaki, A., Zhu, K. J., Hirsch, D. S., Resau, J., Zheng, Y. and Randazzo, P. A.** (2002). ARAP1: a point of convergence for Arf and Rho signaling. *Mol. Cell* **9**, 109-119.

**Moss, J. and Vaughan, M.** (1998). Molecules in the ARF orbit. *J. Biol. Chem.* **273**, 21431-21434.

**Nakano, K., Takaishi, K., Kodama, A., Mammoto, A., Shiozaki, H., Monden, M. and Takai, Y.** (1999). Distinct actions and cooperative roles of ROCK and mDia in Rho small G protein-induced reorganization of the actin cytoskeleton in Madin-Darby canine kidney cells. *Mol. Biol. Cell* **10**, 2481-2491.

**Nie, Z. Z., Hirsch, D. S. and Randazzo, P. A.** (2003). Arf and its many interactors. *Curr. Opin. Cell Biol.* **15**, 396-404.

**Nie, Z. Z., Hirsch, D. S., Luo, R., Jian, X., Stauffer, S., Cremesti, A., Andrade, J., Lebowitz, J., Marino, M., Ahvazi, B. et al.** (2006). A BAR domain in the N Terminus of the Arf GAP ASAP1 affects membrane structure and trafficking of epidermal growth factor receptor. *Curr. Biol.* **16**, 130-139.

**Nobes, C. D. and Hall, A.** (1995). Rho, Rac, and Cdc42 GTPases regulate the assembly of multimolecular focal complexes associated with actin stress fibers, lamellipodia, and filopodia. *Cell* **81**, 53-62.

**Norman, J. C., Jones, D., Barry, S. T., Holt, M. R., Cockcroft, S. and Critchley, D. R.** (1998). ARF1 mediates paxillin recruitment to focal adhesions and potentiates Rho-stimulated stress fiber formation in intact and permeabilized Swiss 3T3 fibroblasts. *J. Cell Biol.* **143**, 1981-1995.

**Oda, A., Wada, I., Miura, K., Okawa, K., Kadoya, T., Kato, T., Nishihara, H., Maeda, M., Tanaka, S., Nagashima, K. et al.** (2003). CrkL directs ASAP1 to peripheral focal adhesions. *J. Biol. Chem.* **278**, 6456-6460.

**Palacios, F. and Souza-Schorey, C.** (2003). Modulation of Rac1 and ARF6 activation during epithelial cell scattering. *J. Biol. Chem.* **278**, 17395-17400.

**Peck, J., Douglas, G., Wu, C. H. and Burbelo, P. D.** (2002). Human RhoGAP domain-containing proteins: structure, function and evolutionary relationships. *FEBS Lett.* **528**, 27-34.

**Powelka, A. M., Sun, J. L., Li, J., Gao, M. G., Shaw, L. M., Sonnenberg, A. and Hsu, V. W.** (2004). Stimulation-dependent recycling of integrin beta 1 regulated by ARF6 and Rab11. *Traffic* **5**, 20-36.

**Puertollano, R., Randazzo, P. A., Presley, J. F., Hartnell, L. M. and Bonifacino, J. S.** (2001). The GGAs promote ARF-dependent recruitment of clathrin to the TGN. *Cell* **105**, 93-102.

**Radhakrishna, H., Klausner, R. D. and Donaldson, J. G.** (1996). Aluminum fluoride stimulates surface protrusions in cells overexpressing the ARF6 GTPase. *J. Cell Biol.* **134**, 935-947.

**Radhakrishna, H., Al-Awar, O., Khachikian, Z. and Donaldson, J. G.** (1999). ARF6 requirement for Rac ruffling suggests a role for membrane trafficking in cortical actin rearrangements. *J. Cell Sci.* **112**, 855-866.

**Randazzo, P. A. and Kahn, R. A.** (1994). GTP hydrolysis by ADP-ribosylation factor is dependent on both an ADP-ribosylation factor GTPase-activating protein and acid phospholipids. *J. Biol. Chem.* **269**, 10758-10763.

**Randazzo, P. A. and Hirsch, D. S.** (2004). Arf GAPs: multifunctional proteins that regulate membrane traffic and actin remodelling. *Cell. Signal.* **16**, 401-413.

**Randazzo, P. A., Nie, Z., Miura, K. and Hsu, V.** (2000a). Molecular aspects of the cellular activities of ADP-ribosylation factors. *Sci. STKE* **59**, RE1.

**Randazzo, P. A., Andrade, J., Miura, K., Brown, M. T., Long, Y. Q., Stauffer, S., Roller, P. and Cooper, J. A.** (2000b). The Arf GTPase-activating protein ASAP1 regulates the actin cytoskeleton. *Proc. Natl. Acad. Sci. USA* **97**, 4011-4016.

**Ren, X. D., Kiosses, W. B. and Schwartz, M. A.** (1999). Regulation of the small GTP-binding protein Rho by cell adhesion and the cytoskeleton. *EMBO J.* **18**, 578-585.

**Ridley, A. J.** (2001). Rho GTPases and cell migration. *J. Cell Sci.* **114**, 2713-2722.

**Rittinger, K., Walker, P. A., Eccleston, J. F., Nurmahomed, K., Owen, D., Laue, E., Gamblin, S. J. and Smerdon, S. J.** (1997a). Crystal structure of a small G protein in complex with the GTPase-activating protein rhoGAP. *Nature* **388**, 693-697.

**Rittinger, K., Walker, P. A., Eccleston, J. F., Smerdon, S. J. and Gamblin, S. J.** (1997b). Structure at 1.65 angstrom of RhoA and its GTPase-activating protein in complex with a transition-state analogue. *Nature* **389**, 758-762.

**Rothman, J. E.** (2002). The machinery and principles of vesicle transport in the cell. *Nat. Med.* **8**, 1059-1062.

**Sabnis, Y., Desai, P. V., Rosenthal, P. J. and Avery, M. A.** (2003). Probing the structure of falcipain-3, a cysteine protease from Plasmodium falciparum: comparative protein modeling and docking studies. *Prot. Sci.* **12**, 501-509.

**Santy, L. C.** (2002). Characterization of a fast cycling ADP-ribosylation factor 6 mutant. *J. Biol. Chem.* **277**, 40185-40188.

**Santy, L. C. and Casanova, J. E.** (2001). Activation of ARF6 by ARNO stimulates epithelial cell migration through downstream activation of both Rac1 and phospholipase D. *J. Cell Biol.* **154**, 599-610.

**Schwartz, M. A. and Ginsberg, M. H.** (2002). Networks and crosstalk: integrin signalling spreads. *Nat. Cell Biol.* **4**, E65-E68.

**Settleman, J., Narasimhan, V., Foster, L. C. and Weinberg, R. A.** (1992). Molecular-cloning of cDNAs encoding the gap-associated protein P190 – implications for a signaling pathway from Ras to the nucleus. *Cell* **69**, 539-549.

**Shattil, S. J. and Newman, P. J.** (2004). Integrins: dynamic scaffolds for adhesion and signaling in platelets. *Blood* **104**, 1606-1615.

**Song, J., Khachikian, Z., Radhakrishna, H. and Donaldson, J. G.** (1998). Localization of endogenous ARF6 to sites of cortical actin rearrangement and involvement of ARF6 in cell spreading. *J. Cell. Sci.* **111**, 2257-2267.

**Stacey, T. T. I., Nie, Z., Stewart, A., Najdovska, M., Hall, N. E., He, H., Randazzo, P. A. and Lock, P.** (2004). ARAP3 is transiently tyrosine phosphorylated in cells attaching to fibronectin and inhibits cell spreading in a RhoGAP-dependent manner. *J. Cell Sci.* **117**, 6071-6084.

**Stouten, P. F. W., Froemmel, C., Nakamura, H. and Sander, C.** (1993). An effective solvation term based on atomic occupancies for use in protein simulations. *Mol. Sim.* **10**, 97-120.

**Turner, C. E., West, K. A. and Brown, M. C.** (2001). Paxillin-ARF GAP signaling and the cytoskeleton. *Curr. Opin. Cell Biol.* **13**, 593-599.

**Verlet, L.** (1967). Computer "experiments" on classical fluids. I. Thermodynamical properties of Lennard-Jones molecules. *Phys. Rev.* **159**, 98-103.

**Watanabe, N., Kato, T., Fujita, A., Ishizaki, T. and Narumiya, S.** (1999). Cooperation between mDia1 and ROCK in Rho-induced actin reorganization. *Nat. Cell Biol.* **1**, 136-143.

**Webb, D. J., Parsons, J. T. and Horwitz, A. F.** (2002). Adhesion assembly, disassembly and turnover in migrating cells – over and over and over again. *Nat. Cell Biol.* **4**, E97-E100.

**Yoon, H.-Y., Bonifacino, J. S. and Randazzo, P. A.** (2005). In vitro assays of Arf1 interaction with GGA proteins. *Methods Enzymol.* **404**, 316-332.

**Zhang, Q., Cox, D., Tseng, C. C., Donaldson, J. G. and Greenberg, S.** (1998). A requirement for ARF6 in Fc gamma receptor-mediated phagocytosis in macrophages. *J. Biol. Chem.* **273**, 19977-19981.

**Zheng, Y., Bagrodia, S. and Cerione, R. A.** (1994). Activation of phosphoinositide 3-Kinase activity by Cdc42Hs binding to P85. *J. Biol. Chem.* **269**, 18727-18730.